INVESTIGATING POSSIBLE INVOLVEMENT OF MIR-125B IN THE E2, NF-κB NETWORK

A THESIS SUBMITTED TO
THE GRADUATE SCHOOL OF NATURAL AND APPLIED SCIENCES
OF
MIDDLE EAST TECHNICAL UNIVERSITY

BY

ESRA YAVUZ

IN PARTIAL FULFILLMENT OF THE REQUIREMENTS
FOR
THE DEGREE OF MASTER OF SCIENCE
IN
BIOLOGY

SEPTEMBER 2015

Approval of the thesis:

INVESTIGATING POSSIBLE INVOLVEMENT OF MIR-125B IN THE E2, NF-κB NETWORK

submitted by **ESRA YAVUZ** in partial fulfilment of the requirements for the degree of **Master of Science in Department of Biology, Middle East Technical University** by,

Prof. Dr. Gülbin Dural Ünver _____
Dean, Graduate School of **Natural and Applied Sciences**

Prof. Dr. Orhan Adalı _____
Head of Department**, Biology**

Assoc.Prof.Dr.A.Elif Erson-Bensan _____
Supervisor, **Biology Dept., METU**

Examining Committee Members:

Prof. Dr Tülin Güray _____
Biology Dept., METU

Assoc. Prof. Dr. A. Elif Erson Bensan _____
Biology Dept., METU

Assoc. Prof. Dr Sreeparna Banerjee _____
Biology Dept., METU

Assoc. Prof. Dr. Tülin Yanık _____
Biology Dept., METU

Prof. Dr. A. Lale Doğan _____
Department of Basic Oncology, Oncology Inst., Hacettepe Uni.

Date: 10.09.2015

I hereby declare that all information in this document has been obtained and presented in accordance with academic rules and ethical conduct. I also declare that, as required by these rules and conduct, I have fully cited and referenced all material and results that are not original to this work.

Name, Last name : Esra Yavuz

Signature :

ABSTRACT

INVESTIGATING POSSIBLE INVOLVEMENT OF MIR-125B IN THE E2, NF-κB NETWORK

Yavuz, Esra

M. S., Department of Biology
Supervisor: Assoc. Prof. Dr. A. Elif Erson Bensan

September 2015, 83 pages

MicroRNAs (miRNAs) play important roles in diverse biological processes and are emerging as key regulators of tumorigenesis and tumor progression. Some miRNAs act as tumor suppressors and are downregulated in cancers such as miR-125b in breast cancer cell lines and tumors. Earlier, we developed a miR-125b expression model system and performed a transcriptomics experiment. Among many indirect targets, ALCAM (activated leukocyte antigen molecule) appeared to be very significantly upregulated in MCF7-125b cells. ALCAM is an NF-κB induced cell-cell contact molecule. Given its significant induction in MCF7-125b cells, we aimed to investigate NF-κB and miR-125b interaction. Interestingly, several studies also linked miR-125b expression and Estrogen (E2) which made us consider whether miR-125b may be a player in the E2-NF-κB network. We investigated nuclear p65, subunit of NF-κB TF (Transcription Factor) and TRAF6 levels, an inducer of NF-κB and a known target of miR-125b in MCF7-125b and T47D-125b cells as well as in E2 treated cells. E2 treated cells demonstrated decreased miR-125a and miR-125b levels both in MCF7 and T47D cells. Accordingly, TRAF6 protein levels increased as a result of E2 treatment in T47D cells. However, we failed to detect TRAF6 in

MCF7 cells. miR- 125b transfected T47D cells also had decreased levels of TRAF6 consistent with miR-125b targeting of TRAF6. NF-κB component nuclear p65 levels also decreased in T47D cells. On the other hand, nuclar localization of p65 also increased in miR-125b transfected MCF7 cells. When MCF7 cells were treated with E2, p65 levels in the nucleus decreased in MCF7 cells. Our data suggests MCF7 and T47D cells are different models of miR-125b expression, possibly due to variations of NF-κB regulatory mechanims. Finally, we detected p65 and TRAF6 levels in miR-125b silenced T47D cells. miR-125b silenced cells had increased TRAF6 and p65 levels, due to decreased miR-125b levels. Our results indicate the complexity of a possible crosstalk between E2, miR-125b and NF-κB and how this complexity may be variable in different cellular backgrounds.

Keywords: miR-125b, breast cancer, NF-κB signalling, p65, TRAF6, estrogen.

ÖZ

E2, NF-κB SİNYAL AĞINDA MİR-125B'NİN OLASI ROLÜNÜN ARAŞTIRILMASI

Yavuz, Esra

Yüksek Lisans, Biyoloji Bölümü
Tez Yöneticisi: Doç. Dr.A.Elif Erson Bensan

Eylül 2015, 83 sayfa

MikroRNAlar (miRNAlar) çeşitli biyolojik süreçlerde önemli roller oynar ve tümörigenezisin ve tümör gelişiminin anahtar düzenleyicileri olarak ortaya çıkmaktadırlar. Bazı miRNAlar tümör baskılayıcı olarak işlev görür ve bazı kanserlerde ifadeleri baskılanır; miR-125b de bu miRNA'lardan biridir ve meme kanseri hücre hatlarında ve tümörlerinde ifadesi baskılanır. Daha önceden, miR-125b ifadesi model sistemi geliştirmiş ve bir transkriptom analizi gerçekleştirmiştik. MCF7-125b hücrelerinde, çok sayıda indirekt hedefler arasında, ALCAM (aktive lökosit antijen molekülü) ifadesinin istatistiksel olarak anlamlı düzeyde arttığı ortaya çıkmıştır. ALCAM, NF-κB sinyal yolağı ile indüklenen bir hücre-hücre adezyon molekülüdür. Biz de, ALCAM'ın MCF7-125b hücrelerindeki ifadesinin artışından yola çıkarak, NF-κB ve miR-125b etkileşimini araştırmayı amaçladık. İlginç bir şekilde, bazı çalışmalarda, miR-125b ifadesinin östrojene (E2) bağlı olarak düzenlendiği gösterilmiştir ve bu da bizi, miR-125b'nin E2- NF-κB sinyal ağında bir rolü olabileceğini düşünmeye sevk etmiştir.

MCF7-125b ve T47D-125b hücrelerinin yanı sıra E2 muamelesi yaptığımız hücrelerde, NF-κB transkripsiyon faktörü olan p65 ve bilinen bir miR-125b hedefi olan NF-κB indüktörü olan TRAF6 seviyelerini ölçtük. E2 muamelesi yaptığımız MCF7 ve T47D hücrelerinde hem miR-125a hem de miR-125b düzeylerinde azalma olduğunu gördük. Aynı zamanda TRAF6 protein seviyeleri T47D hücrelerinde E2 muamelesinin bir sonucu olarak artmıştır. Ancak, MCF7 hücrelerinde TRAF6'yı tespit edemedik. miR-125b transfekte edilmiş T47D hücrelerinde miR-125b'nin TRAF6'yı hedeflemesinden dolayı, TRAF6 seviyesinde azalma gözlemledik. NF-κB sinyal yolağının transkripsiyon faktörü olarak görev yapan p65 düzeyi de T47D hücrelerinde azalmıştır. Öte yandan, miR-125b transfekte edilmiş MCF7 hücrelerinde, hücre çekirdeğindeki p65 seviyesi artmıştır. MCF7 hücreleri, E2 ile muamele edildiği zaman ise, hücre çekirdeğindeki p65 düzeyi azalmıştır. Sonuçlarımız bize, MCF7 ve T47D hücrelerinin, miR-125b ifade seviyeleri açısından, muhtemelen NF-κB sinyal yolağındaki farklı düzenleyici mekanizmalardan dolayı, farklı modeller olduğunu göstermiştir. Son olarak, miR-125b ifadesi susturulmuş T47D hücrelerinde, p65 ve TRAF6 seviyelerini araştırdık. miR-125b'nin ifadesinin susturulmasına bağlı olarak, TRAF6 ve p65 düzeylerinde artış tespit ettik. Sonuçlarımız; E2, miR-125b ve NF-κB sinyal yolağı arasındaki olası bir kompleks ilişkiyi ve kompleks ilişkinin farklı hücresel arkaplan etkilerinden kaynaklanıyor olabileceğini işaret etmektedir.

Anahtar kelimeler: miR-125b, meme kanseri, NF-kB sinyal yolu, p65, TRAF6, östrojen.

To my family

ACKNOWLEDGEMENTS

I would like to thank my supervisor Assoc. Prof. Dr. A. Elif Erson-Bensan for her encouragement and endless support throughout my study.

I would like to thank all my thesis committee members, Assoc. Prof. Dr. Sreeparna Banerjee, Prof.Dr.Tülin Güray, Assoc. Prof. Dr. Tülin Yanık, Prof.Dr. A. Lale Doğan.

I thank all current and previous lab members. And special thanks to Merve Öyken, Tuna Çınkıllı and Gülten Tuncel for their friendship.

My deepest thanks go to Mustafa Çiçek who have been by my side all the time with his endless trust, moral support and patience at every stage of this thesis.

I would like to express my gratitude to my dear mother Feray Yavuz and my dear father Sıdkı Yavuz who raised me to become who I am today.

TABLE OF CONTENTS

LIST OF TABLES

TABLES

LIST OF FIGURES

FIGURES

LIST OF ABBREVIATIONS

ACTB	Beta-actin
Ago 2	Argonaute 2
ALCAM	Activated Leukocyte Cell Adhesion Molecule
ARID3B	AT-rich Intreaction Domain 3
bp	Base pair
DGCR8	DiGeorge syndrome critical region 8
dsRNA	Double stranded RNA
E2	Estrogen
EGFR	Epidermal growth factor receptor
ER	Estrogen receptor
EtOH	Ethanol
Exp-5	Exportin 5
GAPDH	Glyceraldehyde 3-phosphate dehydrogenase
HDAC	Histone deacetylase
Her2	Human epidermal growth factor receptor
miRNA	microRNA
NF-κB	Nuclear factor kappa B
PR	Progesterone receptor
pre-miRNA	Precursor microRNA
pri-miRNA	Primary microRNA
RISC	RNA induced silencing complex
RNA Pol II	RNA polymerase II

SERD	Selective estrogen receptor downregulator
ssRNA	Single stranded RNA
TF	Transcription factor
TFF1	Trefoil factor 1
TNFAIP3	Tumor necrosis factor, alpha- induced protein 3
TRAF6	TNF receptor associated factor 6

CHAPTER 1

INTRODUCTION

1.1. MicroRNAs (miRNAs)

miRNAs or microRNAs were first noticed by Victor Ambros and colleagues, in *C. elegans*, lin-4, a small non-coding RNA that doesn't code for a protein but has important role in controlling timing of larval development [1]. Since then, vast number of miRNAs have been discovered in other organisms such as bacteria, [2], [3], plants [4], mammals [5, 6] and even in viruses [7]. In miRBase release 21.0, June 2014; 35. 828 mature miRNA products have been defined in 223 species. Until now, 2661 human miRNA sequences have been entered to miRBase.

The fact that many miRNAs are conserved among species , indicates that they have an evolutionary conserved role in gene regulation[8], [9], [10]. After the discovery of the critical role of let-7 for larval development regulation in *C.elegans* [11] there have been other studies about miRNA function in cells. Studies showed that miRNAs play critical roles in invertabrate and vertabrate development by regulating proliferation and differentiation of embryonic stem cells, lineage commitment and maturation of tissues [12]. Later work revealed roles of miRNAs in neuronal patterning [13], hematopoiesis lineage commitment [14], tissue homeostasis [15], [16] and apoptosis [17], [18], [19]. miRNAs are also important regulators for metabolism and energy homeostasis [12]. They are important for tissue differentiation involved in production of energy, utilization and storage (e.g., liver, skeletal muscle, adipocytes) [12], regulation of lipid metabolism [20] and insulin release [21].

1.1.1. MiRNA Biogenesis, Mechanism and Function

MiRNAs are ~ 22 nucleotide long small non-coding RNAs [22] which play important roles in gene regulation by targeting mRNAs. MicroRNAs are generally transcribed by RNA polymerase II, followed by endonucleolytic cleavage events [23]. Most of the miRNA genes are found in intergenic regions [24], [25] or in intronic regions. Intronic located miRNAs are found within a host gene, transcribed by the same promoter [26], [27]. However, intergenic miRNAs tend to have their own promoters [28].

Primary miRNAs are similar to mRNA transcripts; they have poly(A) tails and 7-methyl guanylate (m7G) caps [29]. MiRNA biogenesis contains two main cleavage process; firstly nuclear , then cytoplasmic cleavage is done by ribonuclease III endonucleases, Drosha and Dicer [30], [31]. After transcribed by RNA Polymerase II, the resulting transcript is a capped and polyadenylated product [32]. MiRNAs of animals are firstly transcribed as ∼80 nucleotide RNA stem-loop that forms primary miRNA (pri-miRNA) s [32]. Then, these long primary transcripts, pri-miRNAs, are processed into hair-pin shaped pre-miRNAs by nuclear RNase II enzyme Drosha [33]. The intermediate product, precursor miRNA (pre-miRNA) is sent out of the nucleus with the Ran-dependent nuclear transport receptor family protein Exportin-5 (Exp-5) [34], [35]. This pre-miRNA is finally cleaved by cytoplasmic enzyme Dicer [36], [37], [38], [39] into a ∼22-nt long two stranded miRNA. One strand is degraded, but the other one remains as a mature miRNA [31]. The strand which has a less stable 5' end, usually remains as the mature miRNA [40], [41], [42] (Figure 1.1).

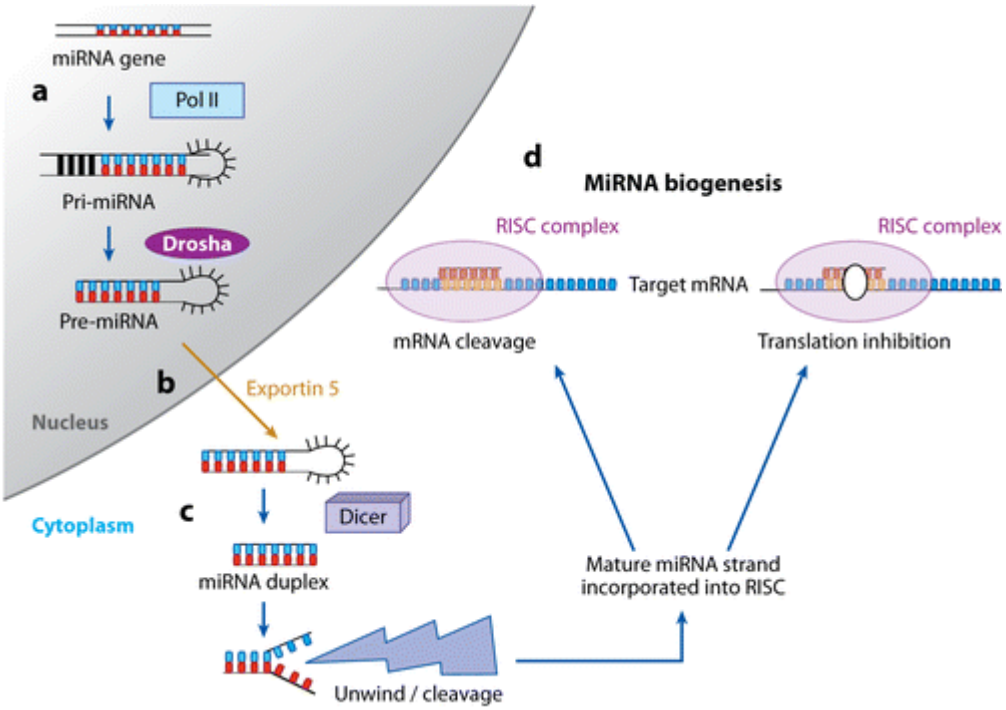

Figure 1.1. MiRNA biogenesis. (a) RNA polymerase II (pol II) transcribes miRNAs into pri-miRNAs, and then they are cleaved by RNase III enzyme Drosha in the nucleus which give rise to pre-miRNA. (b) Pre-miRNA translocates to the cytoplasm via exportin 5 and processed by Dicer. (c) One strand of miRNA duplex (mature miRNA) incorporates with RISC. (d) miRNA guide RISC to cleave mRNA or repress translation (Figure taken from Garzon R, et al. 2009) [42].

MiRNA maturation process shows differences depending upon miRNA location (intergenic or coding-intronic) in the genome [32]. Intergenic miRNAs are transcribed by RNA Pol II and the product is a pri-miRNA [32]. The process of maturation starts with pri-miRNA nuclear cleavage by ‘’microprocessor’’ complex which contains Drosha and RNA-binding protein DiGeorge syndrome critical region gene 8 (DGCR8) [30], [43]. There is evidence showing that some other microprocessor-associated proteins are needed for specific pre-miRNAs during the maturation process [44], [45]. The most accepted model for processing indicates that the recognition of pri-miRNA by DGCR8 leads Drosha to cleave a specific site and form a ~ 60-70 bp pre-miRNA [46], [47], [48]. The resulting pre-miRNA have 5′ phosphate and 3′ hydroxy ends, and two- or three-nucleotide 3′ single-stranded overhanging ends, all of which are characteristics of Drosha cleavage of dsRNA

[49]. So, mature miRNA resides in the 3′ arm of some pre-miRNA and in the 5′ arm in others [49].

Coding-intronic miRNAs are located in introns of protein coding genes and are transcribed as part of the pre-mRNA by Pol II [26]. A relatively novel type of miRNAs, referred as mirtrons, have also been discovered in mammals [50], [51]. pre-mRNA splice sites are appropriately marked and microprocessor selectively cleaves pre-miRNA, at the same time splicing continues normally to generate mature mRNA [51]. This observation proves that the microprocessor complex has an alternative method of recognition that still needs to be investigated from in detail [52], [53], [54].

1.1.2. Target Recognition and Silencing by miRNAs

Activated RISC binding to target mRNA works through classical Watson Crick base-pairing between the 3' UTR of the target and guide strand [55],[56]. The rate of complementary sites between the target and guide strand is important to determine the gene silencing process [57], [58].

One miRNA can regulate various mRNA targets or several miRNAs can together target a single mRNA [6]. Mainly, there are two different silencing mechanisms; translational repression and mRNA cleavage, that can be described as slicer-independent and slicer-dependent silencing respectively [59]. Slicer dependency requires a perfect sequence match between miRNA and target mRNA and means endonuclease cleavage of the mRNA by Ago2 [60]. MRNA degradation (slicer dependent mechanism) and translation inhibition (slicer independent mechanism) both leads to gene expression downregulation. The difference between two processes is that the mRNA degradation is not reversible; but, translation inhibition is reversible [61].

Translational repression occurs by miRNA-RISC binding to 3'UTR (untranslated region) of target mRNA [62], [63]. Perfect binding of miRNA and its target is not

necessary for translational repression [64], [65]. This is generally seen in animals but complete binding of miRNAs to their targets is seen in plants which lead to cleavage of mRNA target [66]. Plant miRNA and target binding occurs by perfect complementarity [67]. Whereas mammalian miRNA-target binding is imperfect except for ‘’seed region’’. Seed region is 7 nucleotide long and begins from the second nucleotide of the mature miRNA. Because of this seed region can be found in many targets, only one miRNA may target many mRNAs [68], [69].

1.1.3. MiRNAs in Cancer

Cancer is a complex and progressive disease that leads normal cells develop genetic alterations which cause neoplastic processes. At the end of these changes, cancer cells have very distinct characteristics like invasion and metastasis, continuous angiogenesis, limitless replicative potential, evading apoptosis, independency of growth signals and insensitivity to growth signals [70].

Cancer initiation and development is associated with deregulation of apoptosis, cell differentiation and proliferation genes. Tumor suppressors and oncogenes are cancer associated genes. While activation of oncogenes causes selective growth advantages which could lead to tumor development, tumor suppressor genes have repressive roles in cell. Both group of genes have regulatory roles in biological processes; so deregulation of their expression leads to cancer [71]. MiRNAs; just as protein coding genes, can have tumor suppressor or oncogene function in cancers [72]. Because miRNAs play essential roles in controlling numerous signaling and regulatory pathways in cell, especially those controlling cell division, proliferation, differentiation and survival [73]. Expression pattern of miRNAs show differences for particular tissues, so their tumor suppressor or oncogenic characteristics differ among tissues [74], [75]. Several mechanisms like mutation, deletion, epigenetic silencing or alterations at miRNA processing induce loss of function of miRNAs [76]. Loss of function of tumor suppressor miRNAs may cause to malignant transformation of a normal cell. The miRNAs are considered oncogenes if their expression increased in tumors. These oncogenic miRNAs are also called oncomirs and they induce tumor

development via suppressing tumor suppressor genes or the genes which control cell differentiation or apoptosis [77], [78].

1.1.4. MiRNA Function in Breast Cancer

Breast cancer is one of the most common cancer types among women and it is a complex disease described by significant genetic changes. Based on their phenotype and gene expression profile, there are six major types of breast cancer. These are tumor enriched with human growth factor receptor 2 (Her2), claudin-low, normal like, basal-like, luminal A and luminal B subtype [79]. Luminal A is the most common subtype and defined by expression of progesterone receptor (PR), estrogen receptor (ER), Bcl-2 and lack of Her2 [80]. The luminal B subtype is defined by the expression of PR, ER and lack of Her2. They can be separated from luminal A subtype based on high Ki67 staining which marks higher proliferation rate [81]. Her2 positive subtype is characterized by high proliferation rate and high Her2 gene expression. Basal-like subtype does not express the three markers (ER, PR and Her2) [81]. In normal-like subtype, ER, PR and Her2 are expressed but absence of expression of EGFR and CK5 [81]. Claudin- low subtype is triple negative and defined by low E-cadherin expression, ocludin and claudin-3,4,7 [82]. Figure 1.2. shows molecular classification of breast cancer.

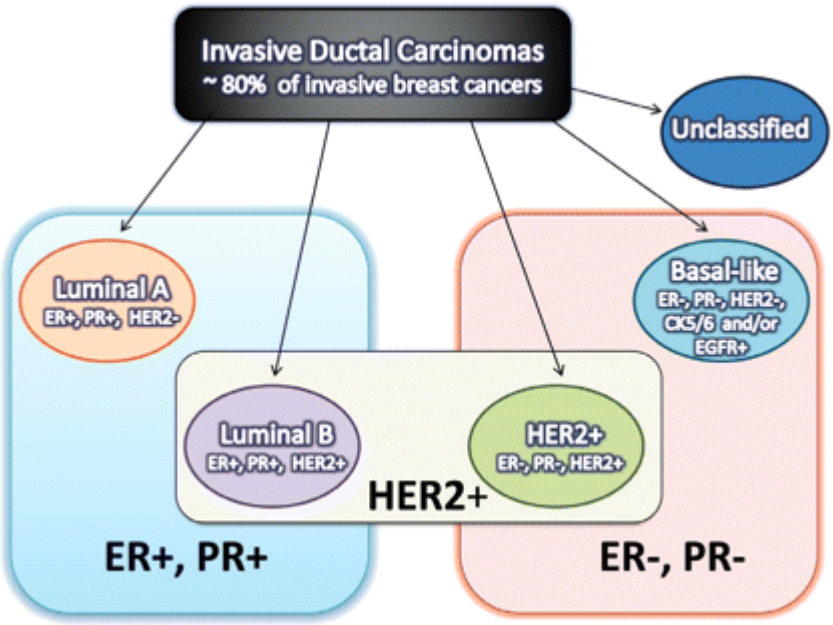

Figure 1.2. Molecular classification of Breast Cancer. Breast cancer subtypes based on their ER, PR, HER2, CK5/6 expression profile (Figure is taken from Labmedicine Volume 41 Number 6- Molecular Classification of Breast Cancer).

These different subtypes are known to have specific miRNA expression patterns [83]. For instance, miR-221, miR-210 and miR-21 are significantly upregulated in triple negative breast cancer; on the other hand miR-122a, miR-145, miR-205 are significantly downregulated [83]. miR-221, miR-210 and miR-21 associated with worse survival rate, so they play an important role in triple negative breast cancers [84]. In an another study, let-7c, miR-199a-3p, miR-146-5p, miR-145, miR-143, miR-127-3p, miR-126 and miR-125b were shown to be upregulated in basal like subtype, but miR-429 and miR-200c are mostly upregulated in luminal subtype [84]. Also, miR-199, miR-145, miR-143, miR-127 and miR-126 levels are significantly upregulated in myoepithelioma compared to basal-like and luminal subtypes. MiR-429 and miR-200c levels were lower in malignant myoepithelioma than basal-like and luminal breast cancer [85].

The most remarkable miRNAs which act as oncogenes expressed in breast cancer cells are miR-10 family [86], miR-21 [87], miR-17-92 cluster [88]. Tumor suppressor miRNAs mostly seen in breast cancer are let-7 family [89], miR-200 family [90] and miR-125b [91], [92], [93]. Thus it is clear that miRNAs in breast cancers have important roles (Figure 1.3).

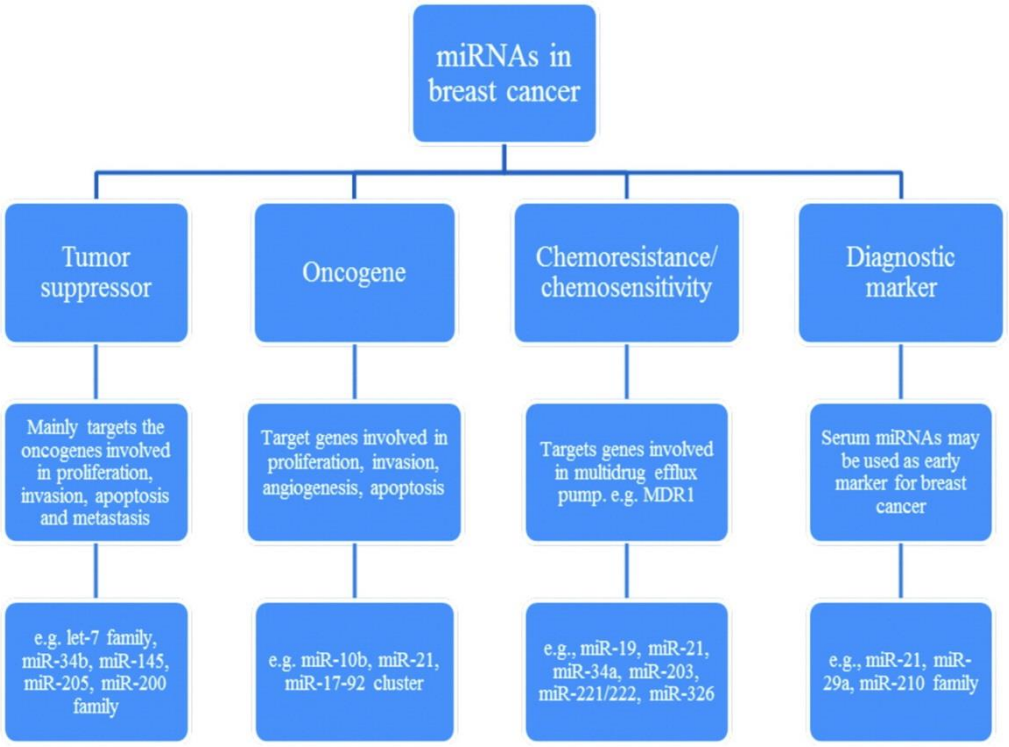

Figure 1.3. Functional classification of miRNAs in breast cancer. (Figure is taken from Role of microRNAs in breast cancer Ramesh Singha & Yin-Yuan Moa) [83].

1.2. MiR-125 Family and Its Expression in Breast Cancer

Lin-4 is among the miRNAs found in *C.elegans* and miR-125b is the human orthologue [94]. *Lin-4* is important in post-embryonic proliferation process and differentiation process in the organism [93]. Human miR-125b expression level is highest in thyroid gland, epididymis, prostate, liver, uterus, ovaries, pituitary gland,

brain, placenta, testes and spleen (http://www.microRNA.org). MiR-125b is a member of miR-125 family, comprise of miR-125a, miR-125b-1 and miR-125b-2. miR-125b-1 and miR-125b-2 precursors are processed and form the same mature miRNA, miR-125b. Even though mature miR-125a and miR-125b sequences are different , they have the same seed region (nucleotides 1-9), so this indicates that they may target same mRNAs [92] (Figure 1.4).

hsa-mir-125a: 5'- UCCCUGAGACCCUUUAAC**C**UGUGA – 3

hsa-mir-125b: 5'- UCCCUGAGACCCU__ AAC**U**UGUGA – 3

Figure 1.4. Mature miR-125a and miR-125b sequences and differences between them.

MiRNA-125b (miR-125b) is deregulated in several different tumors [95]. Interestingly, while miR-125b downregulation in some tumors suggests tumor suppressive potential of miR-125b, upregulation in others indicates that miR-125b may have oncogenic roles [95].

MiR-125a is downregulated in breast cancer, gastric cancer, colorectal cancer, glioblastomas and non-small cell lung cancer (NSCLC) indicating that miR-125a acts as a tumor suppressor for these tumors [95] . Mature miR-125b originates from miR-125b-1 (chromosome 11q24) and miR-125b-2 (chromosome 21q21) [95], [96], [97]. It has been shown that both gene loci are inside fragile sites that are usually deleted in ovary, breast, cervical and lung cancers [95], suggesting loss of function for miR-125b in these tumor types. Downregulation of miR-125b is also seen at other tumor types like; endometrial tumors [96], gliomas [97], Ewing sarcomas [98], osteosarcomas [98], oral squamous cell carcinomas [99], melanomas [100], head and neck tumors [101] (Figure 1.5). Although the molecular mechanisms of miR-125b downregulation are not exactly known, miR-125b promoter hypermethylation which

could lead to supression of miR-125b expression has been shown in some of these cancer types [100], [101].

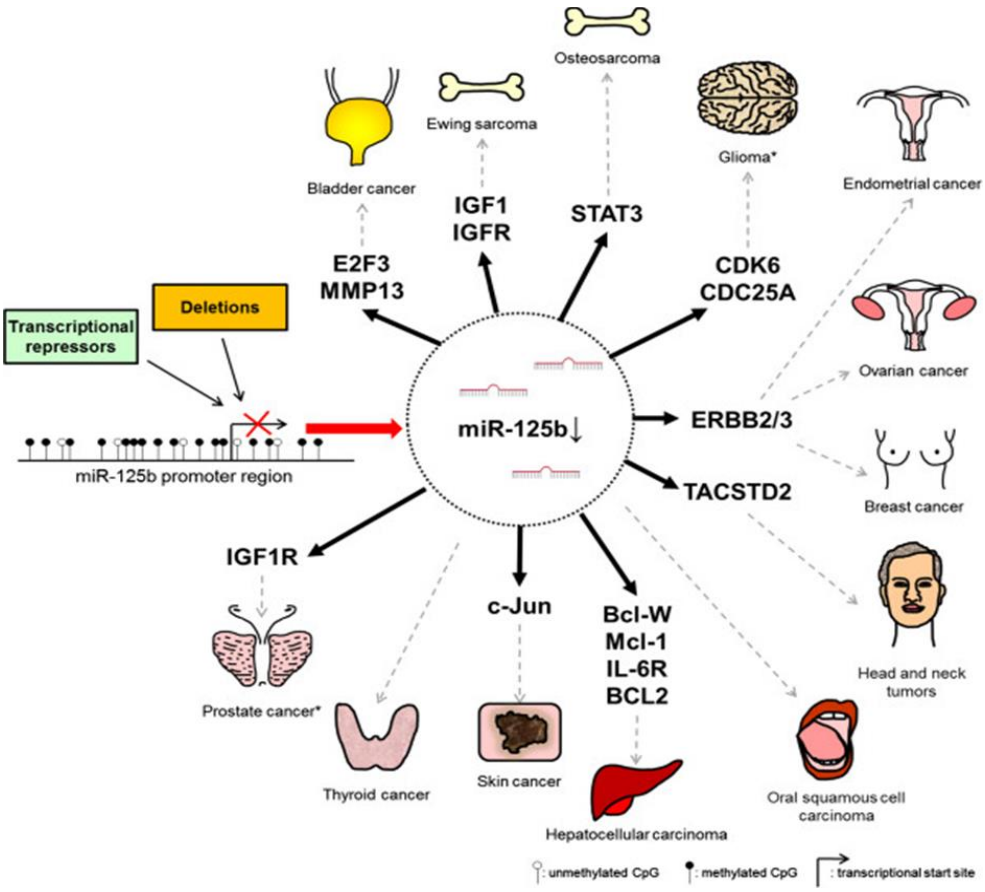

Figure 1.5. Deletions, hypermethylation and androgen signaling reduces miR-125b expression. This causes target mRNAs' upregulation causing indicated tumor types formation. (Figure is taken from Good guy or bad guy: the opposing roles of microRNA 125b in cancer Julia Banzhaf-Strathmann1* and Dieter Edbauer) [102].

MiR-125b has important roles in cellular proliferation, differentiation and apoptosis [103], [104] processes which are all associated with cancer. For instance; p53, which is a tumor suppressor gene controlling the regulation of apoptosis [105], is directly targeted by miR-125b [106]. MiR-125b also targets other mRNAs as cyclin C, cdc25c, Puma and Bak 1 which are cell cycle and apoptosis regulators [104]. Other

cancer related genes are also directly targeted by miR-125b such as HER2/3 in invasive mammary carcinomas such as human epidermal growth factor receptor (Her2 and 3) [107]. These genes are also related with lung, ovarian, salivary, bladder and stomach carcinomas [108]. Extended levels of those genes changes signaling pathways which affect cellular control mechanisms [108].

Downregulation of miR-125b expression in mammary tumors and other cancerous tissues may suppress tumor progression via upregulated p53 expression and possibly others [102]. For breast cancer, due to decreased miR-125b expression, increased expression of miR-125b target EGF receptor family members ERBB2/3 is an important oncogenic driver [109].

ERBB2 and 3 are among the first identified miR-125b targets [110]. Downregulation of miR-125b activates ERBB2/3 expression which enhances cellular proliferation through MAPK signaling pathway and suppress apoptosis through targeting mTOR pathway [110]. Further, miR-125b expression decrease in ERBB2 positive tumors was detected compared to ERBB2 negative breast tumors [111]. ARID3B is another confirmed target of miR-125b in MCF7 cells [89]. ARID proteins are TFs which controls cell growth, development and differentiation [112], mesenchymal transition [113], regulation of actin cytoskeleton organization and cell motility [114]. miR-125b downregulation in breast cancer also activates the expression of EPO (erythropoietin) again raising cellular survival [115]. Also, miR-125b was shown to target ETS1, one of the ETS transcription factor families, in breast cancer [100]; E2F3, a cell cycle regulator, in bladder cancer [116]; a proto-oncogene BCL3 in ovarian cancer [117]. Other upregulated miR-125b targets in breast cancer are multiple epidermal growth factor-like-domains 9 (MEGF9), Glutamyl aminopeptidase (ENPEP), cyclin J (CCNJ) and casein kinase II subunit α (CK2-α) [91]. In addition to direct targets, our group reported indirect/ downstream targets of miR-125b using miR-125b transfected MCF7 cells in a microarray experiment [90]. Majority of gene expression changes are possibly due to downstream and indirect effects of miR-125b expression [90]. Activated leukocyte antigen molecule (ALCAM) was among the significantly increased downstream effectors of miR-125b. ALCAM is an NF-κB induced cell-cell adhesion molecule

[90]. Expression of ALCAM transcript levels were significantly increased upon miR-125b expression in miR-125b transfected MCF7 cells [90].Because ALCAM is important for cell-cell interactions, tightly bound cells via ALCAM possibly have less proliferation rate as detected in MCF7-125b ALCAM expressing cells [90]. On the other hand, there was no ALCAM induction in T47D-125b cells. Unlike MCF7-125b cells, T47D-125b cells also didn't show a decreased proliferation rate, maybe because of different cellular backgrounds [90].

However, for some other types like colorectal cancer [118], gliomas [119], pancreatic cancer [120], gastric cancer [121] , follicular cancer [122] and some leukemias [123] miR-125b upregulation has been reported (Figure 1.6). The reason of these upregulations could be aberrant miRNA expression because of translocations and copy number variations which occur at miRNA loci [124]. In these tumors, miR-125b was shown to target anti-apoptotic proteins [124].

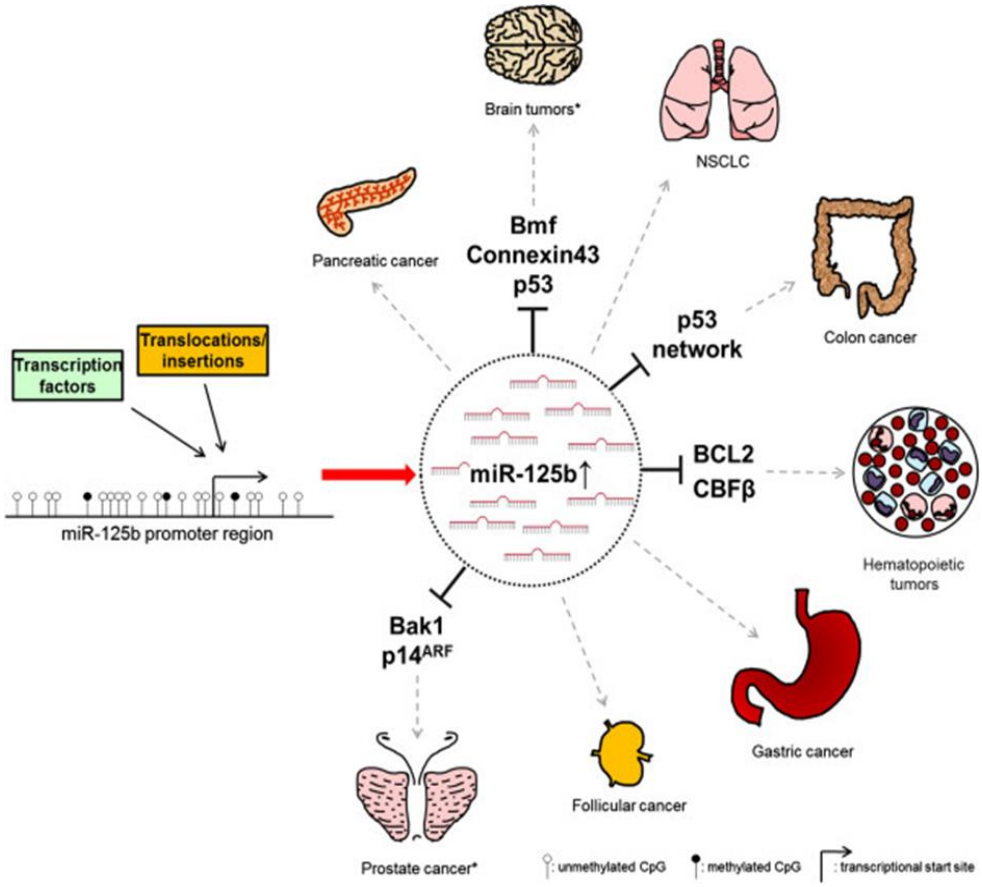

Figure 1.6. Oncogenic potential of miR-125b. Some translocations, insertions and androgen signaling cause miR-125b upregulation. Translational blockage of target mRNAs, leads formation of indicated tumor types.(Figure is taken from Good guy or bad guy: the opposing roles of microRNA 125b in cancer Julia Banzhaf-Strathmann1* and Dieter Edbauer) [102].

1.3. NF-κB transcription factor and Its Role in Cancer

NF-κB (nuclear factor kappa-light-chain-enhancer of activated B cells) pathway is one of the most deregulated pathways in tumor progressing process. So, it is crucial to understand the regulators of this pathway and its relationship with other cancer associated pathways. NF-κB transcription factors family comprises of five members: RelA or p65, RelB, cRel, NFκB1 or p50 and NFBκ2 or p52 [125]. All of these members have highly conserved Rel homology domain at their N-terminus, that is responsible for DNA binding, nuclear translocation, dimerization, and association with NF-κB inhibitor (IκB) proteins [126]. Mature NF-kB proteins forms

homodimers and heterodimers that can bind to DNA [127]. Various stimuli can induce activation of NF-κB like inflammatory cytokines (TNFα, lipopolysaccharide and IL-1), chemicals and growth promoting signals [125]. Activation of NF-κB pathway goes through either the canonical pathway or the noncanonical pathway [128]. In the canonical NF-κB pathway, NF-κB dimers (generally RelA/NFκB1) are kept in the cytoplasm by the inhibitor of NF-κB α-protein (IκBα). After activation, phosphorylation of IκBα is done by a complex comprises of inhibitor of NF-κB kinase 1 (IKK1) (IKKα), IKK2 (IKKβ) and IKKγ. IκB proteins Phosphorylation induces degradation of cytoplasmic inhibitors and promotes NFκB complex translocation into the nucleus [125]. In non-canonical pathway, activation of the p52/RelB NF-κB complex is targeted. This pathway depends mainly on the inducible processing of p100, a molecule functioning as both a RelB-specific inhibitor and the precursor of p52. Another important signaling component for non-canonical pathway is NF-κB-inducing kinase (NIK), which combines signals from TNF receptor family members and activates IκB kinase-α (IKKα), to trigger p100 phosphorylation and processing. The non-canonical (nc) pathway results in processing of the p100 protein to form active p52, that can bind a dimerization partner, mainly RelB, and entering to the nucleus [129].

NF-κB regulates almost every position of tumor biology, such as; progressing of cell survival, stimulation of cell proliferation, metastasis promotion and stimulation of angiogenesis [129]. For breast cancer, NF-κB has roles in the epithelial-mesenchymal transition induction [130]. Recent studies suggests that, self-renewal of breast cancer stem cells are regulated by mammary epithelial NF-κB in a model of Her-2 dependent way [131].

It was demonstrated that NF-κB activation is found mainly in ER-negative breast tumors [132]. Parallel to these results, there is an inversely correlated relationship between NF-κB DNA binding and cellular ER concentration [125]. Furtherway; NF-κB target gene expression is mostly expressed in breast tumors which have low ER target gene expression [133], [134]. Also, in human retinal pigment epithelial cells, Toll-like receptor-4-mediated NF-κB activation is reversed by the estradiol addition,

indicating that the inhibitory crosstalk between these transcription factors is reciprocal [135], [136]. In another study, it was demonstrated that 17β-estradiol (E2) increases p105 subunit levels in MCF7 cells, inhibiting NF-κB activation, because p105 blocks nuclear translocation of NF-κB [137]. Also, ER can interact with transcriptional enhancers or repressors related with NF-κB transcription pathway. ER may compete with NF-κB to bind to transcriptional activators like CREB-binding protein or ER may recruit repressors like glucocorticoid receptor interacting protein 1 to NF-κB complexes [138].

Although most of the studies suggest the negative crosstalk between ER and NF-κB, there are some studies showing a positive cross-talk between them [139], [140]. There may be three main mechanisms: 1) ER-enhanced expression of NF-κB target genes, 2) NF-κB-enhanced expression of ER target genes and 3) an additive effect of both transcription factors [141], [142]. For example, expression of some estrogen responsive genes (like ABCG2 and PTGES) is enhanced by NF-κB because NF-κB stabilizes the binding of ER to its response element [142]. For CCND1, there is a different mechanism between ER and NF-κB. Because CCND1 promotor does not have an estrogen response element, ER should interact with NF-κB proteins which allow the binding of the complex to NF-κB response elements found in the promotor of CCND1. So, this data suggests that NF-κB is crucial to bind ER to the cyclin D1 promoter [143].

There are many studies showing that ER/NF-κB crosstalk could lead to endocrine resistance. Lots of studies focused on NF-κB activation and it's the role in ER positive endocrine resistant breast cancer. To compare tamoxifen-sensitive and tamoxifen-resistant MCF-7 cells, the results indicated that obtaining a resistant phenotype along with elevated NF-κB activity levels [144].

To summarize, all these data suggest that, NF-κB may modulate ER activity, also affect ER positive breast cancer tumors response to endocrine therapy. There are different hypothesis to explain this resistance. Firstly, transrepression of ER by NF-κB may lead ER-positive breast cancer cells losing ER expression and, thus, leads

tumor cells to subpopulation which are endocrine treatment resistant [141]. Secondly, transrepression of NF-κB by ER could lead to resistance to aromatase inhibitors, SERDs (selective estrogen receptor downregulators) or estrogen withdrawal. Elevated ER activation which results from aromatase inhibition or estrogen withdrawal releases NF-κB from the ER-driven inhibition, causing NF-κB-induced tumor progression [141] .

1.4. NF-κB - miR-125b Relationship

The relationship between miRNAs and NF-κB pathway has been studied [145], [146]; pointing out that dysfunction of these interactions may lead to NF-κB associated tumors. For example, miR-125a and miR-125b target TNFAIP3, an inhibitor of NF-κB signaling pathway in lymphomas [147], [148]. Stable expression levels of miR-125a/b in DLBCL (Diffuse Large B Cell Lymphoma) cell lines showed NF-κB function induction, but when miR-125a or miR-125b antagomirs used, via upregulation of TNFAIP3 expression, activity of NF-κB significantly decreased [149], [150]. This indicates that NF-κB may stimulate transcription of miR-125b1, maybe by extend or strengthen some signals by suppressing TNFAIP3 [148]. It was confirmed that DLBCL cells which transfected with miR-125a and/or miR125b have lower expression of TNFAIP3 and higher activity of NF-κB [148].

In an another study, it was demonstrated that BCL3 is important for inducing cell proliferation because it can bind NF-κB p50 and p52 dimers, giving rise to expression of proliferation genes [151]. BCL3 is a miR-125b target and miR-125b is involved in proliferation of OC (ovarian cancer) cells [152], [117]. So, this indicates that, miR-125b controlled proliferation of OC cells through regulation of BCL3 expression [117].

TRAF6 is an important effector in the TLR-mediated NF-κB activation pathway [153]. TRAF6 plays a crucial role in the induction of inflammatory responses via activation of IκB kinases, leading to NF-κB nuclear translocation and activation [154]. It was also shown that miR-125b targets TRAF6 in rat cardiomyoblasts [153]

(Figure 1.7). So that, high levels of miR-125b has an inhibitory role on NF-κB pathway.

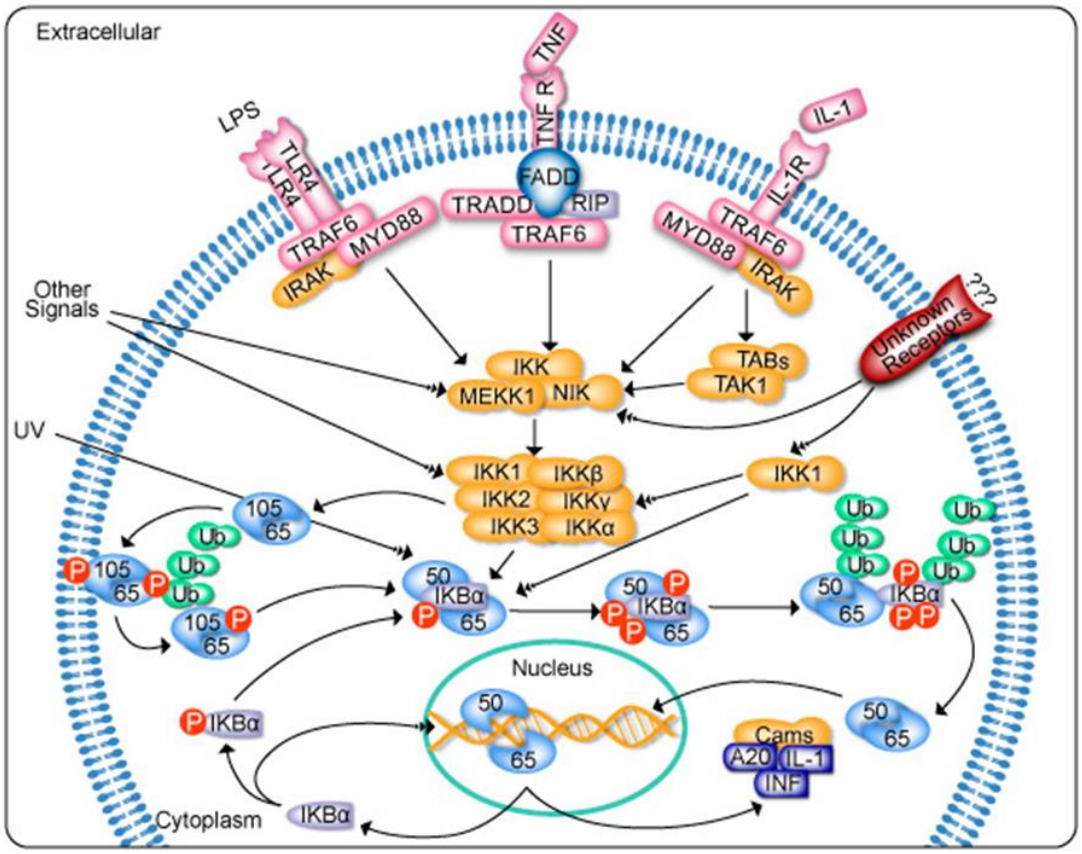

Figure 1.7. NF-κB signalling pathway. The activity of NF-κB is primarily regulated by interaction with inhibitory IκB proteins including IκBa, IκBb, IκBg, IκBe, etc., and also by IκB kinase (IKK). The activated NF-κB complex enters the nucleus to activate target gene expression. (Figure is taken from GeneCopoeia: NF-κB Signaling Pathway 2015).

Interestingly, miR-125b was also linked to both NF-κB and E2 signaling in breast cancers. As previously mentioned, Drosha process pri-miRNAs [155] which is associated with approximately 20 polypeptides, collectively named as the ‘’Drosha microprocessor complex’’ [43]. Drosha complex components p68 and p72 play roles in miRNA processing [156]. Interestingly, p68 and p72 coactivate ERα (Estrogen

Receptor alpha) and increase the transcriptional activity of ERα, via getting interaction with the N terminus of ERα, but not ERβ (Estrogen Receptor beta) [157]. Also, ERα N terminus directly interacts with LXXLL motif of Drosha C terminus [158]. ERα–Drosha interaction, enhanced by E_2 and liganded ERα (E_2-ERα); suppresses the expression of some miRNAs in mouse uterus, through downregulating the Drosha-mediated processing of pri-miRNAs to pre-miRNAs [158]. There is evidence that, E_2-ERα represses the expression of some mature miRNAs, such as miR-125a levels in MCF-7 cells, but does not affect the pre-miR-125a transcription levels [158], [159], [160], [161]. These data shows that suppression of miRNA processing by E2-ERα complex may be associated with its direct interaction with p68/p72 and Drosha [158]. ERβ is not known to interact with Drosha or p68 [162], [163], [164].

To understand whether miRNAs play roles in ER(+) breast cancer progression, the expression of 800 miRNAs was profiled using NanoString in estrogen dependent breast cancer cell line MCF7 and its estrogen independent form MCF7:2A [165]. 78 of these miRNAs were found to be upregulated; including let-7c, miR99a, and miR125b in MCF7:2A cells. These miRNAs are indicated as ER targets in MCF7 cells, and in MCF7:2A cells, ER binding and expression of these miRNAs significantly decreased [165]. Also, it was showed that these miRNAs are expressed at higher levels in luminal A tumors than luminal B tumors and luminal B breast cancers have a worse outcome than luminal A. And within the luminal A subtype, low expression of the let-7c/miR99a/miR125b cluster may cause poor patient outcome. It was found that, let-7c and miR-125b inhibit HER2 protein expression and HER2 protein increase in luminal A tumors lacking expression of these miRNA may cause poor patient outcome. To understand that whether these miRNAs are estrogen regulated, they measured their expression in response to E2 treatment. A 3 hour treatment demonstrated an increase in expression of miR125b [165].

With *in vitro* assays, liganded (estrogen bounded) ERα was demonstrated to inhibit the process of maturation of the miRNAs by interacting with the Drosha complex and so preventing the transition of pri-miRNAs into pre-miRNAs [158]. So, the

regulation of mature and pre-miRNA expression may be post-transcriptional level but not at transcriptional level. It was previously found that p68/p72 interacts with the N-terminal A/B domain of ERα [166]. Because of that, E2-bound ERα regulates the enzymatic function of the Drosha complex by its physical interaction with p68/p72 [158].

1.5. Aim of the Study

Based on our earlier findings that miR-125b transfected cells had different ALCAM levels [100], a target of NF-κB, and that E2 may alter miR-125b levels, we aimed to start investigating whether miR-125b may be a player in the E2- NF-κB network. While the crosstalk between E2 and NF-κB pathways would be expected to be complex, we investigated if miR-125b can be considered as a component of this complex network.

CHAPTER 2

MATERIALS AND METHODS

2.1. Cancer Cell Lines, Cell Culture Conditions and Treatments

MCF7 and T47D cells (Appendix A) were grown in DMEM with Earle's salts and 10% FBS. T47D cells were grown in DMEM with Earle's salts , 10% FBS and 0.1% non-essential amino acids. Media contained 1% Penicillin/Streptomycin (P/S). MCF7-EV, MCF7-125b, T47D-EV and T47D-125b stably transfected cells were generated earlier by our group [100]. T47D-mirzip125b stably transfected cells (miR-125b silenced cells via shRNA) were generated by Merve Öyken. Stable cell lines were maintained with the 0.25 mg/mL Geneticin (Cat#04727894001; Roche Applied Sciences) addition .Cell lines were cultured as monolayers and were incubated at 37°C with 5% CO_2 and 95% humidified air.

For hormone induction experiments, cells were grown in phenol red-free medium containing 10% charcoal stripped FBS (Appendix F), 1% L-glutamine and 1% P/S for 48 hours. Treatments with 10 nM 17 β-Estradiol (E2) (β-Estradiol E2257-1MG; Sigma-Aldrich) or ethanol (vehicle control) for MCF7 and T47D were performed for 12 and 24 hours. 1 μM ICI 182,780 (Cat.# 1047; Tocris Biosciences) pre-treatments were performed 1 hour before E2 treatment for both cell lines.

Cell frozing in liquid nitrogen was done when cells reached approximately 70-80% confluent. Ten or five percent DMSO (dimethyl sulfoxide) (Sigma, Cat# 154938) was added to the media for long term storage of frozen cells. Cell pelletting was done during freezing at 1400 rpm for 5 minutes. Cells were thawed in a 37°C water bath.

2.2. RNA Isolation by Trizol Reagent

DEPC-treated water was used for preparation of all of the solutions used in RNA isolation. 6-well cell culture plates were used to growe cells to 70-75% confluency. Medium was discarded from the wells and 1.1 mL of Isol reagent (Guanidine thiocyanate) from 5 Prime (Cat# 2302700) was used for each well for lysis of the cells. After incubation at room temperature (RT) for 5 minutes, lysates were taken into 1.5mL sterile eppendorf tubes and 510 µl chloroform was added for each tube. Tubes were vigorously shaken for 15 seconds . After incubation at RT for 2-3 minutes, samples were centrifuged at 4500g for 20 minutes at 8°C. After centrifuging, phase seperation was occured and RNA was in the aqueous phase and this aqueous phase was taken to an another 1.5 ml tube. To precipitate RNA, 530 µl of isopropanol addition was done to each RNA containing aqueous phase. The tubes were incubated at RT for 10 minutes then centrifuged at 13000g at 4°C for 20 minutes. After centrifuge, a gel-like RNA pellet was formed. Supernatant was discarded and washing of RNA pellet was done with 75% ethanol by briefly vortexing. Centrigugation was done again at 13000g at 4°C for 10 minutes. Then this step was repeated with %70 ethanol. Ethanol was discarded very well from the tube and samples were left to dry for 15 minutes at RT. Suspension of the pellet was done in 25 µl Molecular grade water. RNA samples were kept at -80°C for long storage.

2.3. RNA Quantity and Quality Determination

RNAs were quantified via NanoDrop ND2000 (Thermo Scientific). RNA sample purity was detected by A260/A280 and A260/A230 ratios. RNA concentration was calculated using the following formula : RNA (µg/mL) = 40 X Dilution Factor X OD260. For all RNA samples, A260/A280 ratio was between 1.8 and 2 and A260/A230 ratio was higher than 1.8 (Appendix B.1.).

2.4.cDNA synthesis

cDNAs synthesis were performed by using synthesized via the RevertAid First Strand cDNA Synthesis Kit (Cat#1622; Life Technologies). Random primers were used for the reaction. Reaction conditions are given in Table 2.1.

Table 2.1. Reverse Transcription Reaction Conditions

RNA	500 ng (1-2 µl
Primer (oligodT or random hexamer)	1 µl
MG water	variable
TOTAL	12 µl
Briefly centrifuged and incubated for 5 minutes at 70 °C.	
5X Reaction Buffer	4 µl
Ribolock RNAse inhibitor	1 µl
dNTP mix	2 µl
RevertAid RT enzyme	1 µl
TOTAL	20 µl
Tubes were incubated for 60 minutes at 42°C; reaction was stopped by heating at 70°C for 5 minutes.	

2.5.DNase I Treatment

DEPC-treated water was used for all the solutions in DNase treatment. Treatment of isolated RNA samples were done using Deoxyribonuclease I (DNase I) from Fermentas (Cat # EN0521) to acquire DNA-free RNA. Reaction components are listed in Table 2.2.

Table 2.2. DNase I reaction mixture

RNA (4-5 ug/µl)	10 µl
10 X Reaction Buffer	10 µl
Dnase I (1u/µl)	2 µl
DEPC water	variable
TOTAL	100 µl

Preparation of this reaction mixture was done on ice and reaction was followed through for 60 minutes at 37°C in a waterbath. 100 µl Phenol: Chloroform: Isoamyl Alcohol (25: 24: 1) was used to stop the reaction. Mixture was mixed by vortexing for 30 seconds then left to incubate on ice for 10 minutes. Then, centrifugation of samples were done for 20 minutes at 14000g at 4°C. After centrifuge, RNA containing upper phase (approximately 80 µl) was taken into a fresh tube. Approximately 240 µl 100% ethanol and 8 µl 3M NaAc was added to RNA containing samples and samples were left to incubate overnight at -20°C. The following day, samples were centrifuged at 14000g for 30 minutes at 4° C. Supernatant was removed and the pellet was washed via 70% ethanol and centrifuged again at 14000g for 15 minutes at 4°C. In the end, 25µL MG Water was used to dissolve pellet.

Absence of DNA contamination was controlled by conventional PCR using GAPDH (Glyceraldehyde 3-phosphate dehydrogenase) specific primers. GAPDH_F: 5'GGGAGCCAAAAGGGTCATCA-3' and GAPDH_R: 5'-TTTCTAGACGGCAGGTCAGGT-3' (product size: 409 bp). PCR conditions were: incubation at 94°C for 10 minutes, 40 cycles of 94°C for 30 seconds, 56°C for 30 seconds, and 72°C for 30 seconds, final extension at 72°C for 10 minutes. For positive control, genomic DNA was used (Appendix B.2.).

2.6.Quantitative RT-PCRs for Detection of Mature miRNAs

For detection of the mature miR-125 levels, Taqman assay kit (Applied Biosystems) was used for PCR amplifications. 2 µl of synthesized cDNA was used in 10 µl PCR containing 2X Taqman PCR mastermix (TaqMan ® Universal PCR Master Mix, Cat#4304437) and 20X miRNA assay mix specific for RNU6B (Cat # 4427975-TM:001093), miR-125b (Cat#4427975-TM:000449) and miR-125a (Cat # 4427975-TM:000448). The qRT-PCRs were performed on Corbett Rotor-Gene 6000 (Qiagen, Corbett, Germany). PCR conditions were: denaturation at 95°C for 15 minutes, then 40 cycles at 95°C for 15 s and 60°C for 60 s. RNAU6B was used as reference gene. To calculate mature miRNA expression levels, ΔΔCt method was used (Livak and Schmittgen 2001). Each experiment was run in 3 technical replicates.

Taqman microRNA assay includes two main steps as shown in Table 2.3. The first step was cDNA synthesis of mature microRNAs by microRNA RT kit; extension by looped primers specific to specific microRNA from 20 ng total RNA of starting material. cDNA synthesis conditions were: 16°C for 30 minutes, 42°C for 30 minutes and 85°C for 5 minutes. The second step was synthesis of second strand of cDNA and PCR amplification of microRNA by using specific primers, Taqman Universal master mix. Following conditions were used: incubation at 95°C for 10 minutes, 40 cycles of 95°C for 10 seconds and 60°C for 1 minutes. Assay results of RT-qPCR are shown in Appendix C.

Table 2.3. cDNA synthesis mixture by TaqMan microRNA RT Kit

dNTP mix (100 mM total)	0.15 µl
Multiscribe RT enzyme (50 U/µL)	1 µl
10X RT Buffer	1.5 µl
RNase inhibitor (20 U/µL)	0.19 µl
DEPC water	4.16 µl
Specific primer mix	3 µl
RNA (20 ng/uL)	5 µl
TOTAL	15 µl

Table 2.4. TaqMan qPCR Reaction Mixture

TaqMan microRNA Assay (20X)	0.5 µl
cDNA	2 µL
TaqMan 2X Universal Master mix	5 µl
DEPC Water	2.5 µl
TOTAL	10 µl

2.7. Protein Isolation and Western Blotting

2.7.1.Nuclear and Cytoplasmic Protein Isolation

Nuclear protein extractions were made by NE-PER Nuclear and Cytoplasmic Extraction Reagents Kit (#78835) (Thermo Scientific) according to the manufacturer's instructions. All the tubes and reagents were kept on ice. All centrifuges was done at 4°C. Trypsin was used to remove adherent cells from culture surface. PBS (phosphate buffered saline) was used twice volume of trpsin to stop the trypsin reaction. Cell pellet was taken to 1.5 ml ependorf tubes and centrifuged at 500 g for 2-3 minutes. Pellet was washed with PBS (phosphate buffered saline) and

centrifuged at 500 g for 2-3 minutes again and supernatant was discarded. 100 µl of CER-I reagent was used per cell pellet. This mixture was vortexed very well for 15 seconds and incubated on ice for 10 minutes. Then, 5.5 µl of CER-II reagent was used per cell pellet. Tubes was vortexed for 5 seconds and incubated on ice for 1 minutes. Following that, pellet was vortexed for 5 seconds again and centrifuged at 16000 g for 5 minutes. After the centrifuge, supernatant which contains cytoplasmic proteins was taken to a cool and fresh tube and stored at -80°C. 50 µl of NER-I solution was added to remained pellet and suspended. Pellet was incubated on ice for 40 minutes and vortexed for 15 seconds every 10 minutes during 40 minutes incubation. After the incubation, pellet was centrifuged for 10 minutes at 16000g. Supernatant which contains nuclear proteins was taken to a cool and fresh tube and stored at -80°C. Pierce BCA Protein Assay Kit (Cat.#23227; Themo Scientific) was used to quantificate lysates.

2.7.2. Isolation of Total Protein

Extraction of total proteins was done by M-PER Mammalian Protein Extraction Reagent (#78501; Thermo Scientific). Cells were washed with PBS twice. M-PER was added on monolayer cells (for T75 flasks 500-1000 µL), twirled via shaker for 15 minutes. Cells were collected by scraper into a eppendorf tube. Then lysates were centrifuged at 14000g for 15 minutes. Supernatants were taken to a new tube and stored at -80° C.

2.7.3. Western Blotting Analysis

Nuclear extract, cytoplasmic extract and total protein extract (50 µg) denaturation were done by 6X Laemmli buffer (Appendix E) at 100°C for 10 minutes and were run on a 8% polyacrylamide gel and transferred onto a nitrocellulose membrane. To detect p65 protein, the blocking of membranes were done with 5% non-fat milk in PBS-T (Phosphate Buffer Saline- Tween) (Appendix E) and were left for overnight incubation with the monoclonal anti-p65 mouse antibody (1:500 dilution; sc-8008, Santa Cruz Biotechnology); then incubated for 1 hour with the secondary anti-mouse

antibody (1:2000 dilution; Santa Cruz Biotechnology). For nuclear protein loading control, Histone deacetylase (HDAC) antibody, (sc-81598, Santa Cruz Biotechnology), was used. 5% non-fat milk in TBS-T (Tris Buffer Saline- Tween) (Appendix E) was used for blocking. Primary antibody was 1:1000 diluted and secondary goat anti-mouse (sc-2005; Santa Cruz Biotechnology) antibody was 1:2000 diluted. To detect nuclear protein purity; GAPDH (Glyceraldehyde 3-phosphate dehydrogenase) antibody (sc-25778; Santa Cruz Biotechnology) was used. %5 BSA in TBS-T was used for blocking. Primary antibody was 1:1000 diluted and secondary mouse anti-rabbit antibody (sc-2357; Santa Cruz Biotechnology) was 1:2000 diluted. Cytoplasmic extracts were used to detect TRAF6 (TNF receptor associated factor 6) antibody (1:200 dilution; ab181622, Abcam). %5 BSA in TBS-T was used for blocking. For loading control, ACTB antibody (1:2000 dilution; sc-47778; Santa Cruz Biotechnology) was used. Proteins were visualized using an enhanced chemiluminescence kit (Cat#32132; ECL Plus; Pierce) according to the manufacturer's instructions.

2.8. Analysis of *TFF1* Expression Levels

TFF1 (trefoil factor 1) is a protein encoded by *TFF1* gene (NM_003225) (also called *pS2* gene) and known as an E2 induced gene [167]. TFF1 expression was controlled by conventional PCR as a positive control to confirm the E2 treatment efficiency. Following primers were used; TFF1_F: 5'-CCATGGAGAACAAGGTGATCTGC-3' and TFF1_R: 5'GTCAATCTGTGTTGTGAGCCGAG-3' (product size: 399 bp). PCR conditions were as follows: incubation at 94°C for 10 minutes, 25 cycles of 94°C for 30 seconds, 56°C for 30 seconds, and 72°C for 30 seconds, and final extension at 72°C for 5 minutes.

CHAPTER 3

RESULTS AND DISCUSSION

3.1. Role of miR-125b in NF-κB Signaling Pathway

As one of the most downregulated miRNAs, mir-125b, is predicted to be an important tumor suppressor in breast cancer [89], [90]. In a transcriptome analysis performed in our laboratory, we detected various indirect targets of miR-125b in MCF7-125b cells. One of those was ALCAM, an NF-κB induced cell adhesion protein. In MCF7-125b cells, both ALCAM mRNA and protein levels were significantly upregulated, suggestive of altered NF-κB activity. Interestingly, we detected no increase in ALCAM levels in T47D-125b cells, suggesting that we had 2 different miR-125b expression models. The fact that MCF7-125b cells had decreased proliferation rates compared to EV cells only, supported this observation.

3.1.1. Detection of miR-125a and miR-125b Expression Levels

To better understand the difference between MCF7 and T47D miR-125b transfected cell lines; at first, we measured basal miR-125b expression levels in untransfected cells (Figure 3.1). We demonstrated that, miR-125b levels were downregulated in both cells compared to normal breast. This was expected, and in agreement with our previous analysis.

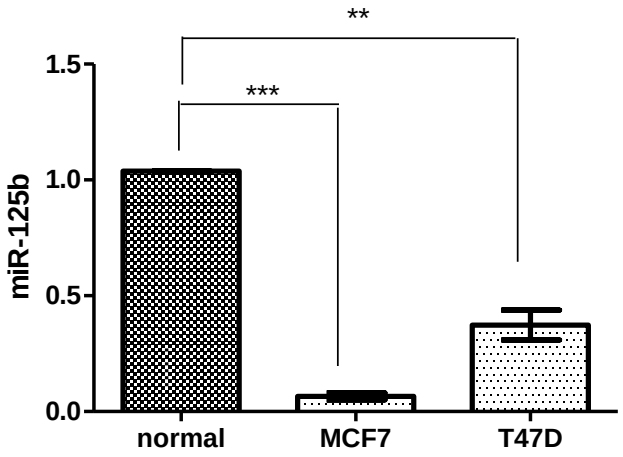

Figure 3.1. Expression levels of miR-125b in MCF7 and T47D cell lines. MiR-125b expression levels of MCF7 and T47D cells were detected by TaqMan qPCR assay. Analysis was performed 2 independent times. Commercial normal breast total RNA was used for normalization. Quantification was done using the reaction efficiency correction and ΔΔCq method. One-way ANOVA with Tukey's multiple comparison post test was performed using GraphPad Prism (California, USA). ** ($p \leq 0.01$), and *** ($p \leq 0.001$) indicates statistical significance.

Next, we confirmed miR-125b levels in the 2 model systems; first model was the stably 125b transfected MCF7 cells, second model was the stably miR-125b transfected T47D cells generated by previous members of our lab (Figure 3.2.a and Figure 3.2.b).

a) b)

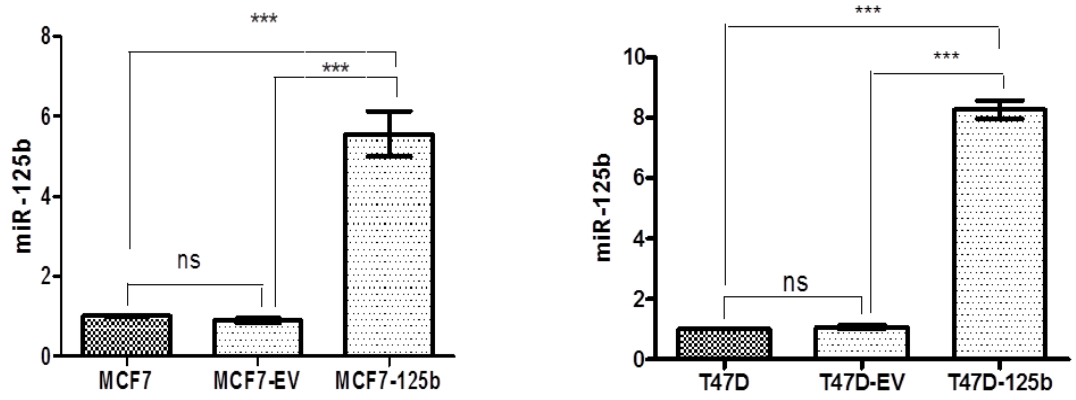

Figure 3.2. Confirmation of stable transfection of miR-125b. Restoration of miR-125b expression was detected by TaqMan qPCR assay a) in MCF7-125b transfected cells and b) in T47D-125b transfected cells compared to their EV transfected and untransfected forms. Each experiment was repeated 2 independent times. The baseline for the control samples was set to 1. miR-125b expression of transfected cells was normalized to untransfected cellsQuantification was done using the reaction efficiency correction and ΔΔCq method. One-way ANOVA with Tukey's multiple comparison post test was performed using GraphPad Prism (California, USA). *** ($p \leq 0.001$) indicates statistical significance.

Stable transfection of miR-125b indeed, increased the miR-125b epression in MCF7 and T47D cells, as expected, confirming the validity of our models.

3.1.2. p65 Protein Levels Changes Upon miR-125b Overexpression

After confirming our model systems, we then decided to start investigating the difference between MCF7-125b and T47D-125b cells. Given that earlier experiments [90] showed significant activation of ALCAM, an NF-κB target, we then looked at NF-κB activation in our model systems. We measured p65 protein levels in both cells as an indicator of NF-κB activation. p65 is a subunit of NF-κB transcription complex, that plays a crucial role in immune and inflamatory responses. Since the activation of this pathway is associated with the intracellular localization of the NF-

κB complex, the nuclear localization of p65 is commonly used as a parameter of activation [167]. Figure 3.3 shows western blotting results in MCF7 and T47D cells and their 125b transfected forms. MCF7- 125b transfected cells showed an approximately 3 fold increase of p65 protein levels; whereas T47D-125b transfected cells showed decreased levels of p65.

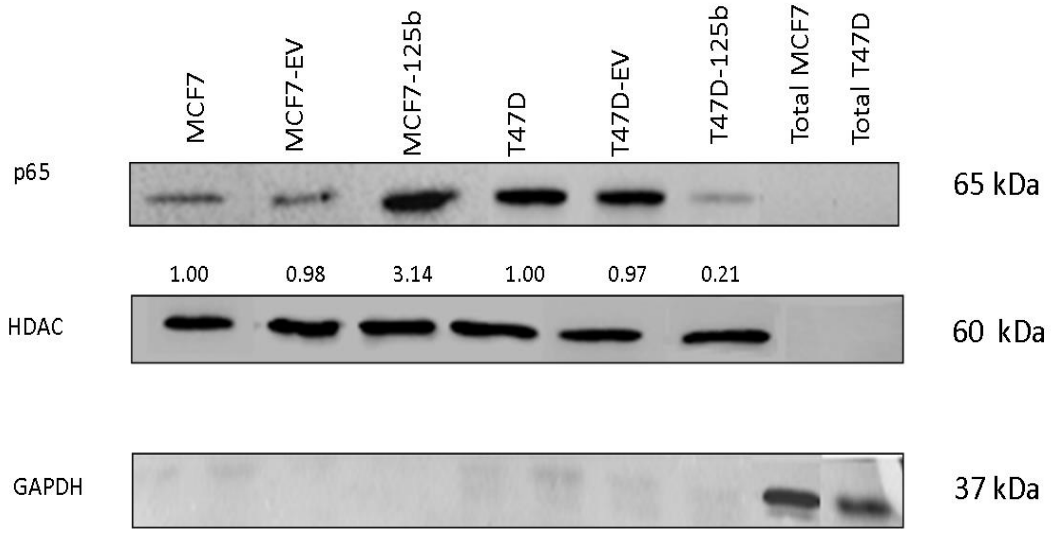

Figure 3.3. Nuclear p65 levels in miR-125b models. As an indicator of NF-κB activity, p65 protein levels were quantified by western blotting for mir-125b transfected cells using nuclear extracts . HDAC antibody was used to test equal loading of nuclear proteins. Lack of cytoplasmic GAPDH was detected by GAPDH antibody. Total protein extracts was loaded to confirm to detect efficiency of GAPDH antibody. Image J program was used for quantification of the bands. Fold increases are indicated below the bands.

To understand why MCF7 and T47D cells have different p65 levels in miR-125b transfected cells, we turned to potential miR-125b targets that have roles in the NF-κB pathway. A known target of miR-125b is actually TRAF6 [168], an inducer of NF-κB [170]. Interestingly, in T47D cells, miR-125b expression indeed resulted with decreased TRAF6 expression, consistent with decreased p65 levels in T47D-125b cells (Figure 3.4).

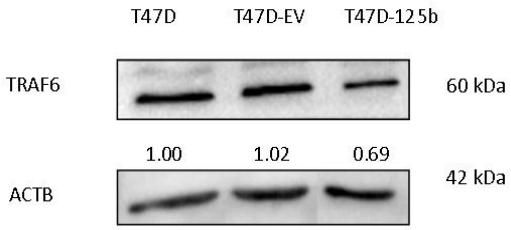

Figure 3.4. Western blot analysis of TRAF6 protein in T47D cells. TRAF6 protein levels were quantified in T47D cells by western blot analysis, using 50 µg of cytoplasmic extracts. Beta actin (ACTB) was used for loading control. Image J program was used for quantification of the bands. Fold increases are indicated below the bands.

To our surprise, we failed to detect significant expression of TRAF6 in MCF7 cells (Figure 3.5).

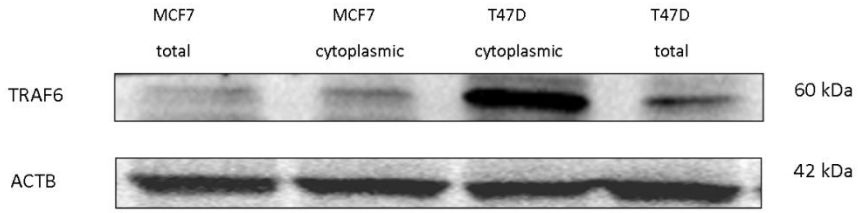

Figure 3.5. Western blot analysis of TRAF6 expression in MCF7 cells. 50 µg of total and cytoplasmic extracts of MCF7 and T47D cells used to quantify TRAF6 protein levels. Beta actin was used for loading control. Image J program was used for quantification of the bands. Fold increases are indicated below the bands.

3.2. miR-125b Expression Levels Upon E2 Treatment

3.2.1. E2 Treatments and Its Effect on miR-125b Maturation Process

To continue addressing the difference in MCF7 and T47D cells in terms of p65 levels; we then turned to the E2 signalling pathway. The reason for choosing the E2 pathway over other pathways to modulate NF-κB was because a study suggested E2 induced downregulation of miR-125b, which led to an increase in TNFAIP3 levels and decreased levels in p65 [169]. TNFAIP3 is a protein which is known to suppress NF-κB activation by inhibiting IKKs [169].

To test whether E2 has any effect on miR-125a and miR-125b expression, first MCF7 and T47D cells were grown in phenol red-free medium containing %10 dextran-coated-charcoal stripped FBS for 48 hours, then added either ethanol or 10 nM E2 for 12 and 24 hours. Next, we isolated RNA, synthesized cDNA and performed TaqMan RT-PCR. TFF1 is an known E2 upregulated gene [167]. The efficiency of E2 treatment was confirmed with the induced expression of TFF1 in E2 treated samples (Figure 3.6).

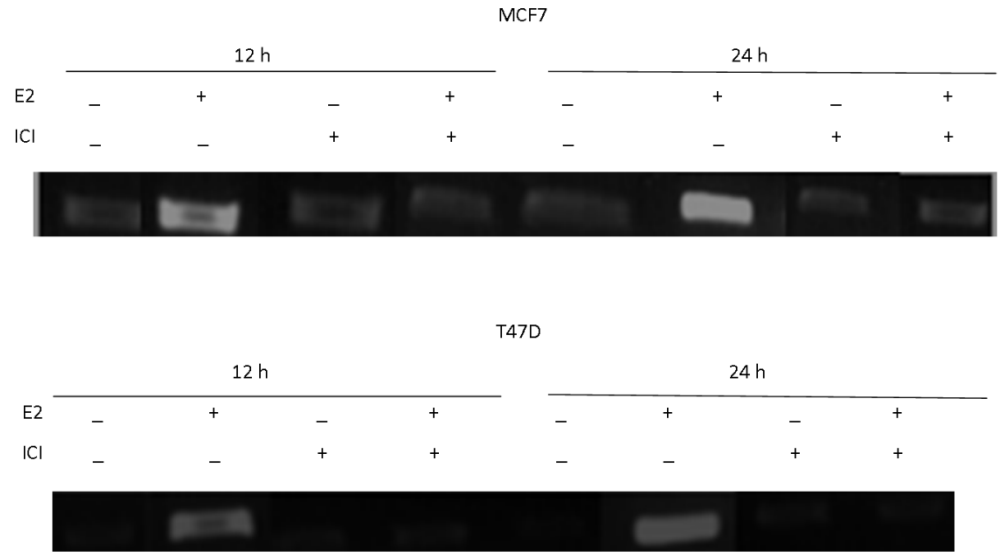

Figure 3.6. TFF1 expression control. MCF7 and T47D cells were grown in phenol red-free medium containing 10% dextran-coated-charcoal stripped FBS, pre-treated with 1 μM ICI for 1 hour, then with 10 nM E2 for 12 and 24 hours. Ethanol was used as vehicle control. E2 treatment caused induced expression of TFF1 gene.

We detected nearly 2 fold reduction in the mature levels of miR-125a and miR-125b in both cell lines upon E2 treatment (Figure 3.7).

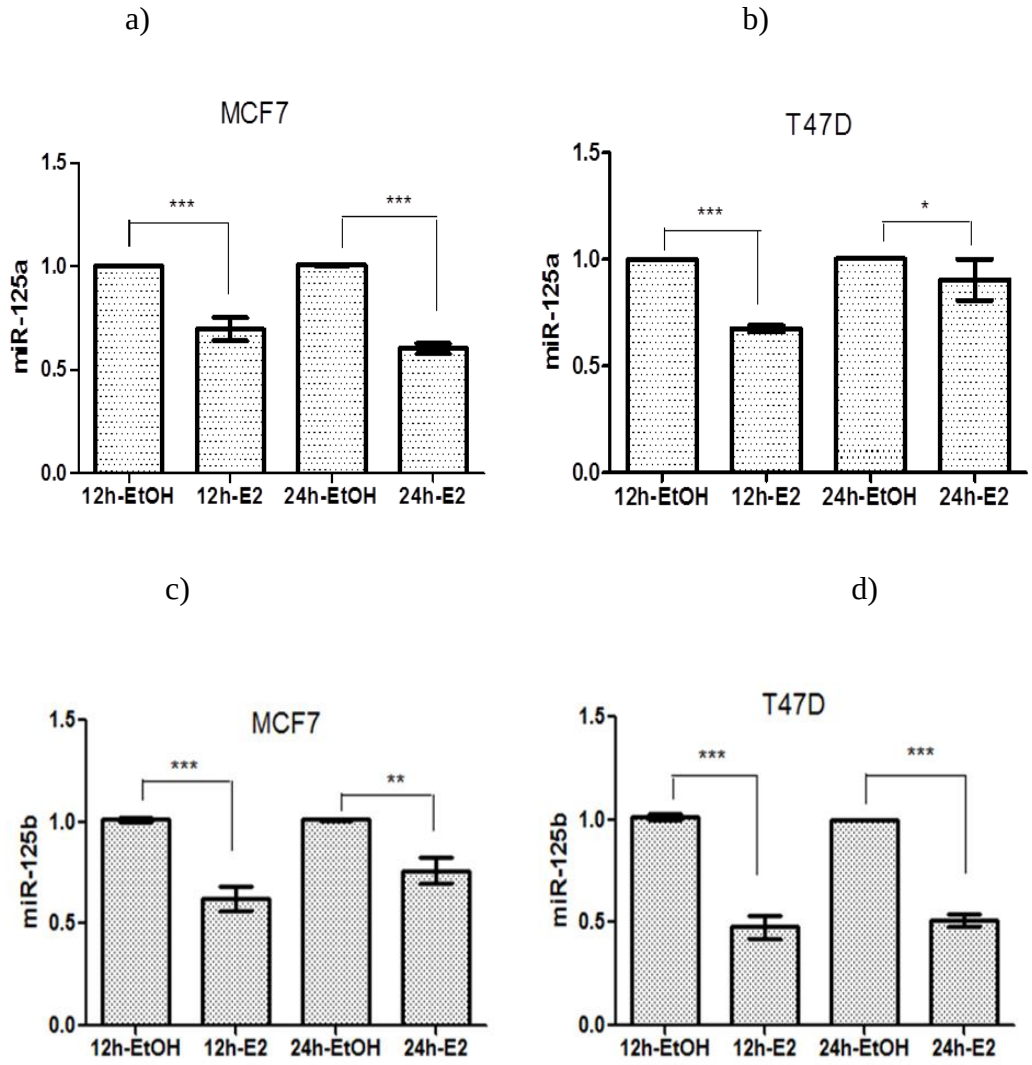

Figure 3.7. Mature miR-125a and mir-125b expression upon E2 treatment. MCF7 and T47D cells were grown in phenol red-free medium containing 10% dextran-coated-charcoal stripped FBS, then treated with 10 nM E2 for 12 and 24 hours. Ethanol was used as vehicle control. a) miR-125a levels upon treatment in MCF7 cells. b) miR-125a levels upon E2 treatment in T47D cells. c) miR-125b levels upon E2 treatment in MCF7 cells. d) miR-125b levels upon E2 treatment in T47D cells. Relative expression of mature miR-125a and miR-125b expression levels were determined by TaqMan RT-qPCR assay. For each experiment, 2 biological replicates were used. TaqMan qpCR assay was performed with 3 technical replicates for each experiment. The baseline for the control treated samples was set to 1. Every treated sample were normalized to its ethanol control at that time point. Quantification was done using the reaction efficiency correction and ΔΔCq method. One-way ANOVA with Tukey's multiple comparison post test was performed using GraphPad Prism (California, USA). * ($p \leq 0.05$), ** ($p \leq 0.01$), and *** ($p \leq 0.001$) indicates statistical significance.

To confirm the effects are due to the presence of ERα (Estrogen Receptor alpha), we treated cells with ICI 182,780 (Tocris Biosciences), an antagonist of ER (Figure 3.8.). For MCF7 and T47D cells, we saw decreased levels of miR-125a and miR-125b expression for E2 treated samples. E2 with prior ICI treatment failed to cause a decrease in miR-125a and miR-125b levels, suggesting the downregulation to be ER specific.

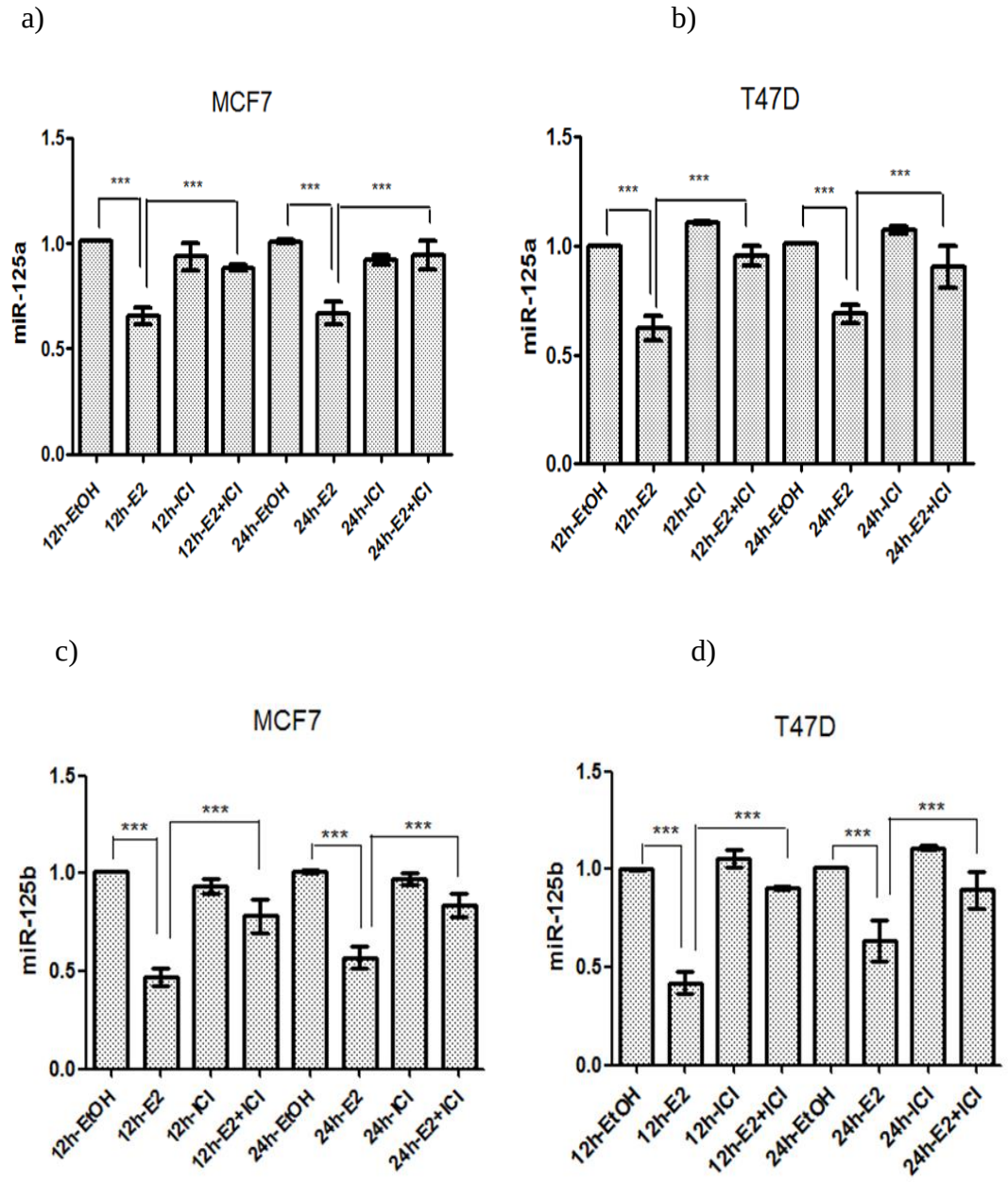

Figure 3.8. Mature miR-125a and mir-125b expression upon E2 and ICI treatments. MCF7 and T47D cells were grown in phenol red-free medium containing 10% dextran-coated-charcoal stripped FBS, pre-treated with 1 μM ICI for 1 hour, then with 10 nM E2 for 12 and 24 hours. Ethanol was used as vehicle control. Relative expression of mature miR-125a and miR-125b expression levels were determined by TaqMan RT-qPCR assay. a) miR-125a levels upon E2 and ICI treatments in MCF7 cells. b) miR-125a levels upon E2 and ICI treatments in T47D cells. c) miR-125b levels upon E2 and ICI treatments in MCF7 cells. d) miR-125b levels upon E2 and ICI treatments in T47D cells. For each experiment, 2 biological replicates were used. TaqMan qpCR assay was performed with 3 technical replicates for each experiment. The baseline for the control treated samples was set to 1. Every treated sample were normalized to its ethanol control at that time point. Quantification was done using the reaction efficiency correction and ΔΔCq method. One-way ANOVA with Tukey's multiple comparison post test was performed using GraphPad Prism (California, USA). *** ($p \leq 0.001$) indicates statistical significance.

3.2.2. p65 Levels Change Upon E2 Treatment

After demonstrating that mature miR-125a and miR-125b levels were decreased by E2, we investigated NF-κB activation using the E2 treated cells. We performed western blotting to detect nuclear p65 levels in T47D and MCF7 cells (Figure 3.9). We saw approximately 2.5-3 fold increase of p65 levels in T47D cells after 24 hour E2 treatment, but there was no change after 12 hours. Interestingly, we saw a reduction in nuclear p65 levels when cells were treated with ICI alone. Considering that cells were grown in charcoal stripped medium lacking E2, and the validity of TFF1 PCR results, our expectation was to see similar protein levels in E2(-) ICI(-) cells.

These results suggested that we might have had some estrogenic contribution of serum if our charcoal stripping was not efficient.

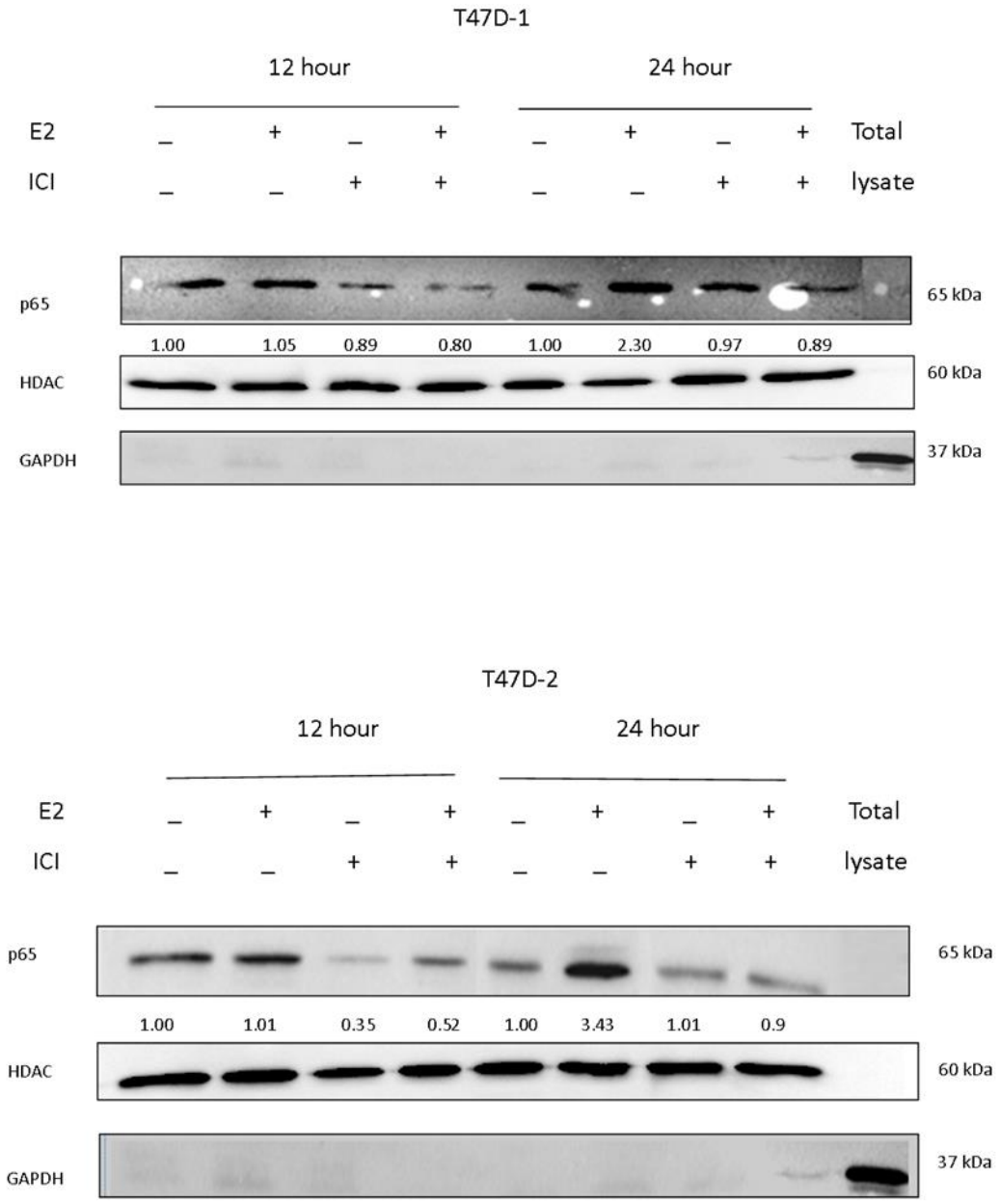

Figure 3.9. Nuclear p65 levels in T47D cells upon E2 and ICI treatments. 50 µg of nuclear lysates of E2 and ICI treated T47D cells were used for western blotting. T47D cells were grown in phenol red-free medium containing 10% dextran-coated-charcoal stripped FBS, pre-treated with 1 µM ICI for 1 hour, then with 10 nM E2 for 12 and 24 hours. HDAC antibody was used to test equal loading of nuclear proteins. Lack of cytoplasmic contamination was detected by cytoplasmic GAPDH esxpression. Total protein extracts was loaded to confirm to detect efficiency of GAPDH antibody. Image J program was used for quantification of the bands. Fold increases are indicated below the bands. T47D-1 and T47D-2 indicate biological replicates.

MCF7 cells, on the other hand, showed an inverse pattern of p65 expression levels due to E2. There was a decrease in p65 levels after 12 hour of E2 treatment (Figure 3.10).

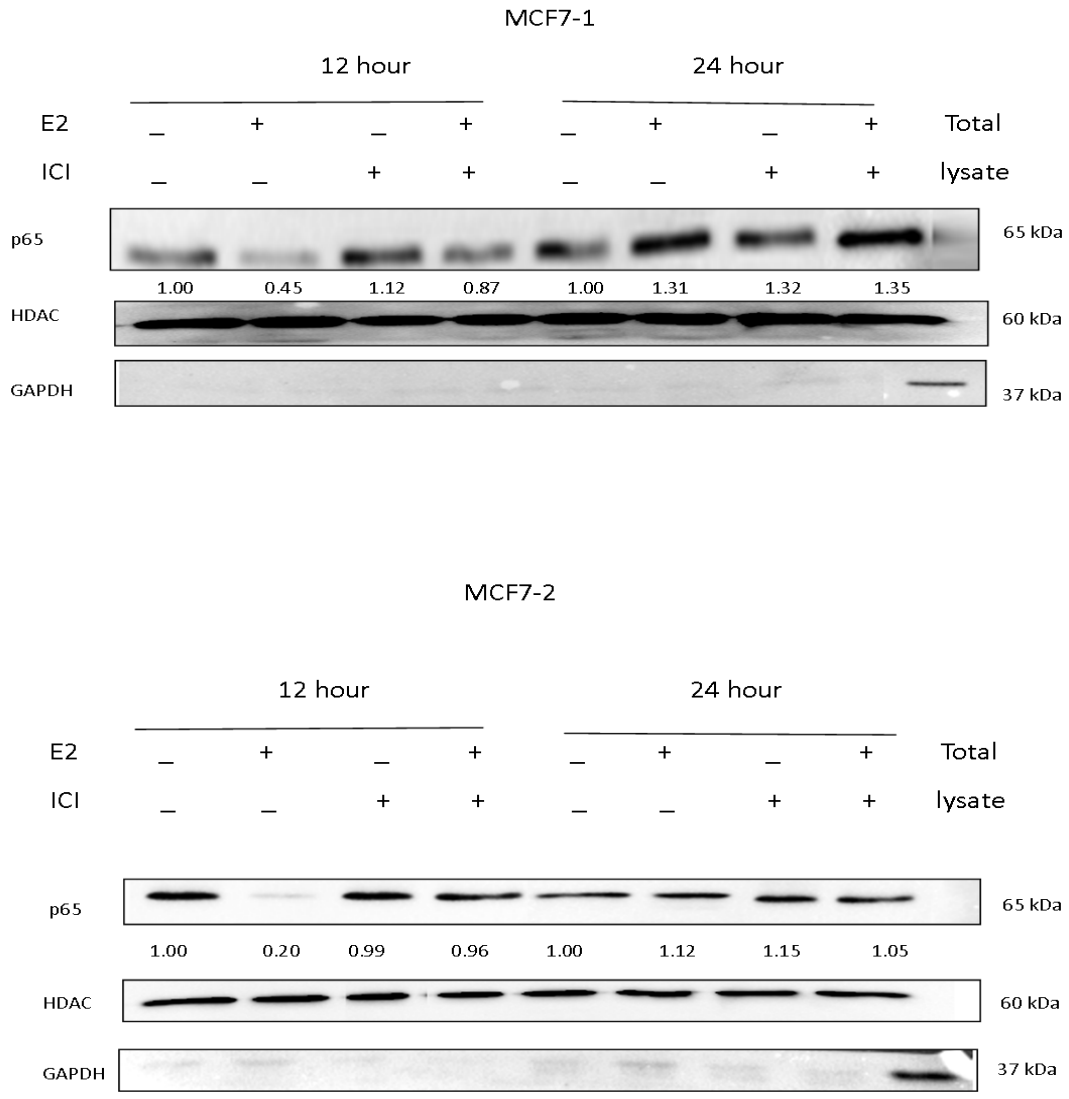

Figure 3.10. Nuclear p65 levels in MCF7 cells upon E2 and ICI treatments. 50 µg of nuclear lysates of E2 and ICI treated MCF7 cells were used for western blotting. MCF7 cells were grown in phenol red-free medium containing 10% dextran-coated-charcoal stripped FBS, pre-treated with 1 µM ICI for 1 hour, then with 10 nM E2 for 12 and 24 hours. HDAC antibody was used to test equal loading of nuclear proteins. Lack of cytoplasmic contamination was detected by cytoplasmic GAPDH expression. Total protein extracts was loaded to confirm to detect efficiency of GAPDH antibody. Image J program was used for quantification of the bands. Fold increases are indicated below the bands. MCF7-1 and MCF7-2 indicate biological replicates.

As expected, ICI alone pre-treatment and E2(-) ICI(-) cells had similar p65 levels, confirming ER involvement. Next, to answer why these 2 cell lines had different

levels of p65 in response to E2, we tested whether TRAF6 levels changed after E2 treatment. We performed a western blot for E2 and ICI treated T47D cells. Parallel to the increase of p65 levels , we saw an increase in TRAF6 levels for T47D cells after 24 hours of E2 treatment. (Figure 3.11).

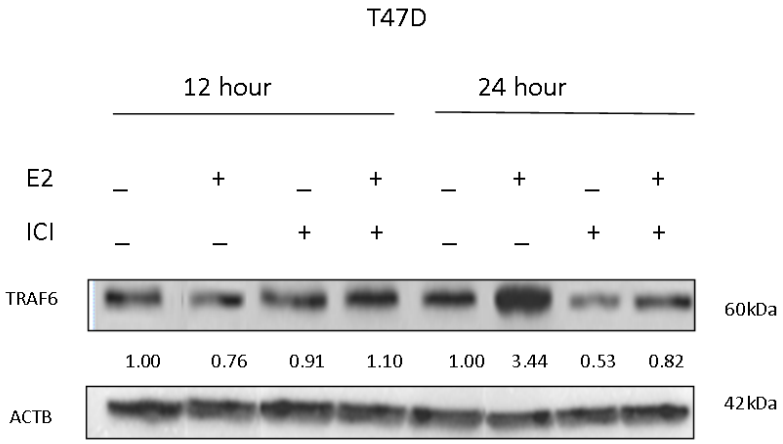

Figure 3.11. TRAF6 levels upon E2 and ICI treatments in T47D cells. 50 µg of cytoplasmic extracts of E2 and ICI treated T47D cells were used for western blotting. T47D cells were grown in phenol red-free medium containing 10% dextran-coated-charcoal stripped FBS, pre-treated with 1 µM ICI for 1 hour, then with 10 nM E2 for 12 and 24 hours. B-actin antibody was used to test equal loading. For the band quantification, Image J program was used. Fold increases are written below the bands.

Because TRAF6 is an inducer of NF-κB activity, this result suggested that decreased miR-125b levels led to an increase in TRAF6 and eventually increased p65 levels in T47D cells. As described earlier, MCF7 cells lack detectable levels of TRAF6. It is also of interest to note that only after 24 hours, we saw an increase in TRAF6. This result may suggest involvement of secondary, tertiary or even later response elements. Currently, the explanation of why p65 levels increase in response to E2 lacks for MCF7 cells. But in MCF7 cells, after 12 hours of E2 treatment, p65 levels were low. This could be due to the fact that TRAF6 is not as ubiqutiously expressed in MCF7 cells as in T47D cells. This suggests, presence of other NF-κB modulator pathways or different miR-125a and miR-125b basal levels in MCF7 and T47D cells.

Then our next step was to investigate specifity of this observation. We already had T47D miR-125b silenced cells (T47D-mirzip125b) in our laboratory. After confirming the silencing (Figure 3.12), we detected p65 and TRAF6 levels in T47D cells with miR-125b aiming shRNA oligos (Figure 3.13).

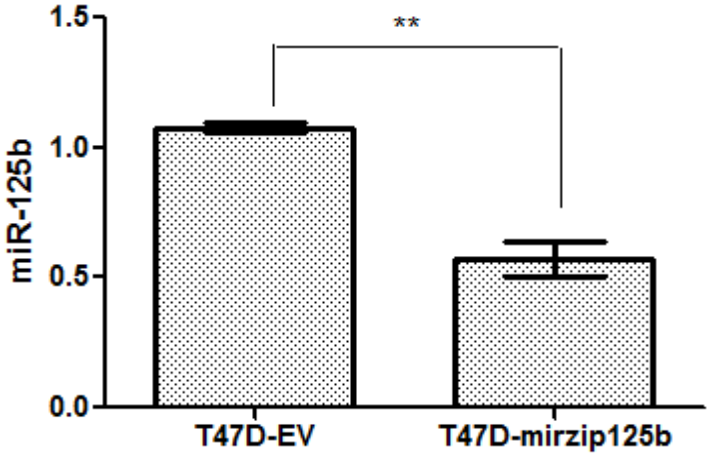

Figure 3.12. Confirmation of miR-125b silencing in T47D cells. Silencing of miR-125b expression was detected by TaqMan qPCR assay in T47D-mirzip125b transfected cells compared to their EV transfected forms. Each experiment was repeated 2 independent times. The baseline for the control samples was set to 1. miR-125b expression of miR-125b silenced cells was normalized to EV transfected cells. Quantification was done using the reaction efficiency correction and ΔΔCq method. One-way ANOVA with Tukey's multiple comparison post test was performed using GraphPad Prism (California, USA). ** ($p \leq 0.01$) indicates statistical significance.

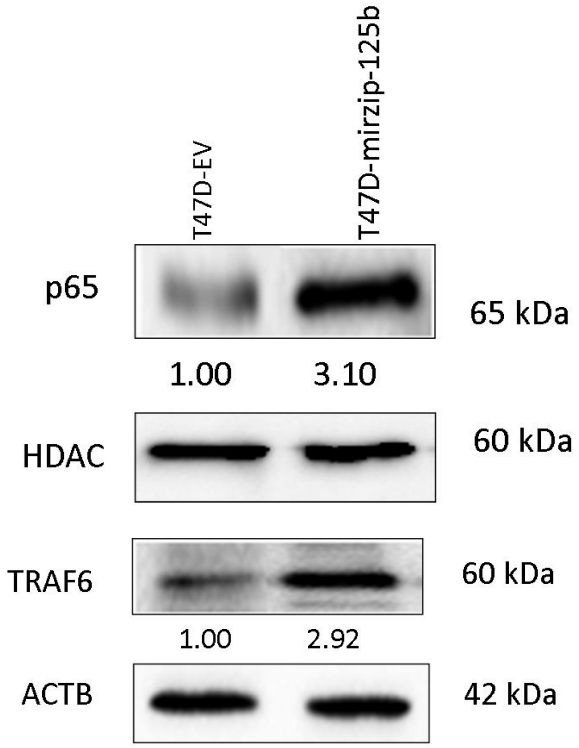

Figure 3.13. p65 and TRAF6 levels of miR-125b silenced T47D cells. 50 µg of nuclear extracts of miR-125b silenced T47D cells (T47D-mirzip125b) and were used for western blotting of p65 protein and 50 µg of cytoplasmic extracts miR-125b silenced T47D cells were used for western blotting of TRAF6 protein. HDAC antibody was used to test equal loading of nuclear extracts and ACTB antibody was used to test equal loading of cytoplasmic extracts. For the band quantification, Image J program was used. Fold increases are indicated below the bands.

Compared to T47D-EV cells, miR-125b silenced cells had increased TRAF6 and p65 levels. However we lack a plausible explanation to how p65 and miR-125b are interconnected in MCF7 cells.

CHAPTER 4

CONCLUSION

miR-125b is downregulated in breast cancers and therefore accepted as a tumor suppressor. We previously detected various indirect targets of miR-125b in a cell line that was stably transfected with miR-125b. One of those was ALCAM, an NF-κB induced cell adhesion protein. In MCF7-125b cells, both ALCAM mRNA and protein levels were significantly upregulated suggesting altered NF-κB activity. However, we detected no increase in ALCAM levels in T47D-125b cells. Mature miR-125b levels are low in both T47D and MCF7 cells compared to normal breast, but high levels of miR-125a were observed in T47D cells but not in MCF7 cells. Considering that both miR-125a and miR-125b target similar RNAs. miR-125a level differences of MCF7 and T47D cells may explain the difference of ALCAM expression levels in T47D and MCF7 cells. Moreover, our results suggested ALCAM transcriptional regulation to be more complex than we initially predicted.

Here, by using expression analysis, changing levels of p65, an NF-κB component were shown upon E2 treatment and miR-125b downregulation in breast cancer cells. TRAF6 is a miR-125b target and we showed that TRAF6 levels decreased when T47D cells were transfected with miR-125b. As an important inducer of NF-κB pathway, TRAF6 levels are in positive correlation with p65 levels . When miR-125b levels increase, TRAF6 is targeted and it can not induce IKKs to phosphorylate NF-κB inhibitor IκB, so NF-κB complex does not translocate to the nucleus to activate transcription.

To further understand role of miR-125b in NF-κB pathway regulation, we stimulated changes of miR-125b levels using E2. E2 has an inhibitory role on miR-125b maturation process in MCF7 and T47D cells. miR-125b expresssion was suppressed

in MCF7 and T47D cells after E2 treatment. Then we measured p65 levels in these cells. For T47D cells, we showed that there is an increase in p65 levels and TRAF6 levels upon E2 treatment. When miR-125b levels decrease in response to E2 treatment; TRAF6 is less targeted and it activates NF-κB pathway, so we see an increase in p65 levels in T47D cells. But interestingly, we showed that MCF7 cells response differently. Although, miR-125b expression is suppressed by E2 , there is a decrease in p65 levels. MCF7 cells does not have or have very low levels of TRAF6 protein, but other regulators of NF-κB pathway may affect the activation process of NF-κB.

Then, to understand whether miR-125b has a direct or indirect role in NF-κB pathway, we used miR-125b silenced T47D cells for detecting p65 and TRAF6 levels. As we expected, we saw increased levels of miR-125b target TRAF6, upon miR-125b silencing. Also we observed that p65 levels were increased parallel to increased TRAF6 levels. These results indicates that, miR-125b regulates NF-κB pathway activation, targeting TRAF6 and also other unidentified miR-125b targets.

When we treated MCF7 cells with E2, miR-125b was downregulated and we saw decreased levels of p65 after 12 hours of E2 treatment. In contrast, T47D cells showed an inverse pattern of these observations. There was a decrease in p65 levels in miR-125b transfected T47D cells and we saw increased levels of p65 upon miR-125b downregulation when we treated T47D cells with E2 for 24 hours. These results emphasized different cellular backgrounds of MCF7 and T47D cells. Possible relationship of E2, miR-125b, and NF-κB is illustrated in Figure 4.1.

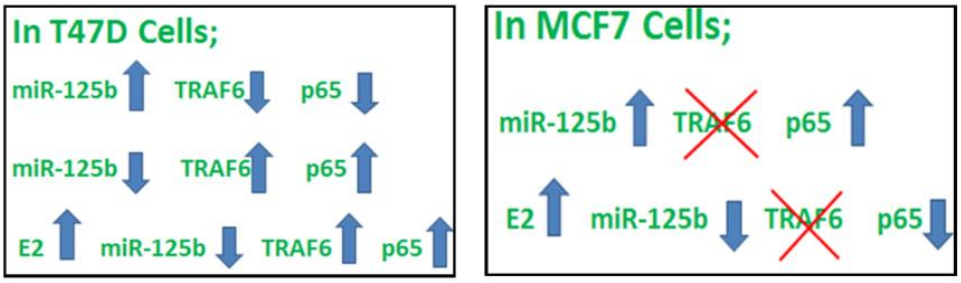

Figure 4.1. MiR-125b, E2 and p65 levels.

Considering that miR-125a and miR-125b target similar mRNAs, our future studies will include detecting p65 and TRAF6 levels in miR-125a transfected and also miR-125a silenced MCF7 and T47D cell lines. Endogenous levels of miR-125a levels in T47D cells may explain the ALCAM and p65 expression difference in MCF7 and T47D cells. It will also be important to consider other NF-κB pathway regulators in terms of ER relevance as well as miR-125a and miR-125b. Unraveling E2, miR-125b and NF-κB relationship will hopefully help studies to explain the endocrine therapy resistance in some patients.

REFERENCES

1. Lee RC, Feinbaum RL, Ambros V. The C. elegans heterochronic gene lin-4 encodes small RNAs with antisense complementarity to lin-14. Cell. 1993;75(5):843-54. PubMed PMID: 8252621. eng.

2. Furuse Y, Finethy R, Saka HA, Xet-Mull AM, Sisk DM, Smith KLJ, et al. Search for MicroRNAs Expressed by Intracellular Bacterial Pathogens in Infected Mammalian Cells. PLoS One. 2014;9(9). PubMed PMID: 25184567. eng.

3. Tjaden B, Goodwin SS, Opdyke JA, Guillier M, Fu DX, Gottesman S, et al. Target prediction for small, noncoding RNAs in bacteria. Nucleic Acids Res. 2006;34(9):2791-802. PubMed PMID: 16717284. Pubmed Central PMCID: 1464411. eng.

4. Jones-Rhoades MW, Bartel DP, Bartel B. MicroRNAS and their regulatory roles in plants. Annu Rev Plant Biol. 2006;57:19-53. PubMed PMID: 16669754. Epub 2006/05/04. eng.

5. Meunier J, Lemoine F, Soumillon M, Liechti A, Weier M, Guschanski K, et al. Birth and expression evolution of mammalian microRNA genes. Genome Res. 23. United States2013. p. 34-45.

6. Bartel DP. MicroRNAs: genomics, biogenesis, mechanism, and function. Cell. 2004;116(2):281-97. PubMed PMID: 14744438. eng.

7. Boss IW, Plaisance KB, Renne R. Role of virally-encoded microRNAs in herpesvirus biology. Trends Microbiol. 2009 Dec;17(12):544-53. PubMed PMID: 19828316. Pubmed Central PMCID: 2802859. eng.

8. Loh YHE, Yi SV, Streelman J. Evolution of MicroRNAs and the Diversification of Species. Genome Biol Evol. 2011;3:55-65. PubMed PMID: 21169229. Pubmed Central PMCID: 3017390. eng.

9. The deep evolution of metazoan microRNAs. 2015.

10. Berezikov E. Evolution of microRNA diversity and regulation in animals. Nature Reviews Genetics. 2011 2011-11-18;12(12):846-60. en.

11. Reinhart BJ, Slack FJ, Basson M, Pasquinelli AE, Bettinger JC, Rougvie AE, et al. The 21-nucleotide let-7 RNA regulates developmental timing in Caenorhabditis elegans. Nature. 2000 Feb 24;403(6772):901-6. PubMed PMID: 10706289. Epub 2000/03/08. eng.

12. Sun W, Julie Li YS, Huang HD, Shyy JY, Chien S. microRNA: a master regulator of cellular processes for bioengineering systems. Annu Rev Biomed Eng. 2010 Aug 15;12:1-27. PubMed PMID: 20415587. Epub 2010/04/27. eng.

13. Johnston RJ, Hobert O. A microRNA controlling left/right neuronal asymmetry in Caenorhabditis elegans. Nature. 2003 2003-12-14;426(6968):845-9. en.
14. Chen C-Z, Li L, Lodish HF, Bartel DP. MicroRNAs Modulate Hematopoietic Lineage Differentiation. 2004 2004-01-02. en.

15. Rodriguez A, Vigorito E, Clare S, Warren MV, Couttet P, Soond DR, et al. Requirement of bic/microRNA-155 for Normal Immune Function. 2007 2007-04-27. en.

16. Devier DJ, Lovera JF, Lukiw WJ. Increase in NF-κB-sensitive miRNA-146a and miRNA-155 in multiple sclerosis (MS) and pro-inflammatory neurodegeneration. Front Mol Neurosci. 2015;8. PubMed PMID: 25784854. Pubmed Central PMCID: 4345893. eng.

17. Baehrecke EH. Autophagic programmed cell death in Drosophila. Cell Death & Differentiation. 2003 2003-09-01;10(9):940-5. en.

18. Cimmino A, Calin GA, Fabbri M, Iorio MV, Ferracin M, Shimizu M, et al. miR-15 and miR-16 induce apoptosis by targeting BCL2. Proc Natl Acad Sci U S A. 2005;102(39):13944-9. PubMed PMID: 16166262. eng.

19. Othman N, Nagoor NH. The role of microRNAs in the regulation of apoptosis in lung cancer and its application in cancer treatment. Biomed Res Int. 2014;2014:318030. PubMed PMID: 24999473. Pubmed Central PMCID: PMC4068038. Epub 2014/07/08. eng.

20. Krutzfeldt J, Rajewsky N, Braich R, Rajeev KG, Tuschl T, Manoharan M, et al. Silencing of microRNAs in vivo with 'antagomirs'. Nature. 2005;438(7068):685-9. PubMed PMID: 16258535. eng.

21. van de Bunt M, Gaulton KJ, Parts L, Moran I, Johnson PR, Lindgren CM, et al. The miRNA Profile of Human Pancreatic Islets and Beta-Cells and Relationship to Type 2 Diabetes Pathogenesis. PLoS One. 2013;8(1). PubMed PMID: 23372846. eng.

22. Ambros V. The functions of animal microRNAs. Nature. 2004;431(7006):350-5. PubMed PMID: 15372042. eng.

23. Macfarlane LA, Murphy PR. MicroRNA: Biogenesis, Function and Role in Cancer. Curr Genomics. 2010 Nov;11(7):537-61. PubMed PMID: 21532838. Pubmed Central PMCID: PMC3048316. Epub 2011/05/03. eng.

24. Lagos-Quintana M, Rauhut R, Lendeckel W, Tuschl T. Identification of novel genes coding for small expressed RNAs. Science. 2001;294(5543):853-8. PubMed PMID: 11679670. eng.

25. Lau NC, Lim LP, Weinstein EG, Bartel DP. An abundant class of tiny RNAs with probable regulatory roles in Caenorhabditis elegans. Science. 2001;294(5543):858-62. PubMed PMID: 11679671. eng.

26. Rodriguez A, Griffiths-Jones S, Ashurst JL, Bradley A. Identification of mammalian microRNA host genes and transcription units. Genome Res. 2004;14(10A):1902-10. PubMed PMID: 15364901. eng.

27. Ying SY, Chang CP, Lin SL. Intron-mediated RNA interference, intronic microRNAs, and applications. Methods Mol Biol. 2010;629:205-37. PubMed PMID: 20387152. Epub 2010/04/14. eng.

28. Saini HK, Griffiths-Jones S, Enright AJ. Genomic analysis of human microRNA transcripts. Proc Natl Acad Sci U S A. 104. United States2007. p. 17719-24.

29. Cullen BR. Derivation and function of small interfering RNAs and microRNAs. Virus Res. 2004;102(1):3-9. PubMed PMID: 15068874. eng.

30. Denli AM, Tops BB, Plasterk RH, Ketting RF, Hannon GJ. Processing of primary microRNAs by the Microprocessor complex. Nature. 432. England2004. p. 231-5.

31. Lee Y, Jeon K, Lee JT, Kim S, Kim VN. MicroRNA maturation: stepwise processing and subcellular localization. EMBO J. 2002 Sep 2;21(17):4663-70. PubMed PMID: 12198168. Pubmed Central PMCID: PMC126204. Epub 2002/08/29. eng.

32. Lee Y, Kim M, Han J, Yeom KH, Lee S, Baek SH, et al. MicroRNA genes are transcribed by RNA polymerase II. EMBO J. 2004;23(20):4051-60. PubMed PMID: 15372072. eng.

33. Lee Y, Ahn C, Han J, Choi H, Kim J, Yim J, et al. The nuclear RNase III Drosha initiates microRNA processing. Nature. 2003;425(6956):415-9. PubMed PMID: 14508493. eng.

34. Valencia-Sanchez MA, Liu J, Hannon GJ, Parker R. Control of translation and mRNA degradation by miRNAs and siRNAs. Genes Dev. 2006;20(5):515-24. PubMed PMID: 16510870. eng.

35. Bohnsack MT, Czaplinski K, Gorlich D. Exportin 5 is a RanGTP-dependent dsRNA-binding protein that mediates nuclear export of pre-miRNAs. RNA. 2004 Feb;10(2):185-91. PubMed PMID: 14730017. Pubmed Central PMCID: PMC1370530. Epub 2004/01/20. eng.

36. Bernstein E, Caudy AA, Hammond SM, Hannon GJ. Role for a bidentate ribonuclease in the initiation step of RNA interference. Nature. 2001 Jan 18;409(6818):363-6. PubMed PMID: 11201747. Epub 2001/02/24. eng.

37. Grishok A, Pasquinelli AE, Conte D, Li N, Parrish S, Ha I, et al. Genes and mechanisms related to RNA interference regulate expression of the small temporal RNAs that control C. elegans developmental timing. Cell. 2001;106(1):23-34. PubMed PMID: 11461699. eng.

38. Ketting RF, Fischer SE, Bernstein E, Sijen T, Hannon GJ, Plasterk RH. Dicer functions in RNA interference and in synthesis of small RNA involved in developmental timing in C. elegans. Genes Dev. 2001 Oct 15;15(20):2654-9. PubMed PMID: 11641272. Pubmed Central PMCID: PMC312808. Epub 2001/10/20. eng.

39. Knight SW, Bass BL. A role for the RNase III enzyme DCR-1 in RNA interference and germ line development in Caenorhabditis elegans. Science. 2001;293(5538):2269-71. PubMed PMID: 11486053. eng.

40. Khvorova A, Reynolds A, Jayasena SD. Functional siRNAs and miRNAs exhibit strand bias. Cell. 2003;115(2):209-16. PubMed PMID: 14567918. eng.

41. Schwarz DS, Hutvagner G, Du T, Xu Z, Aronin N, Zamore PD. Asymmetry in the assembly of the RNAi enzyme complex. Cell. 2003;115(2):199-208. PubMed PMID: 14567917. eng.

42. Garzon R, Calin GA, Croce CM. MicroRNAs in Cancer. Annu Rev Med. 2009;60:167-79. PubMed PMID: 19630570. Epub 2009/07/28. eng.

43. Gregory RI, Yan KP, Amuthan G, Chendrimada T, Doratotaj B, Cooch N, et al. The Microprocessor complex mediates the genesis of microRNAs. Nature. 2004;432(7014):235-40. PubMed PMID: 15531877. eng.

44. Michlewski G, Guil S, Semple CA, Caceres JF. Posttranscriptional regulation of miRNAs harboring conserved terminal loops. Mol Cell. 2008;32(3):383-93. PubMed PMID: 18995836. eng.

45. Guil S, Caceres JF. The multifunctional RNA-binding protein hnRNP A1 is required for processing of miR-18a. Nat Struct Mol Biol. 2007;14(7):591-6. PubMed PMID: 17558416. eng.

46. Zeng Y, Yi R, Cullen BR. MicroRNAs and small interfering RNAs can inhibit mRNA expression by similar mechanisms. Proc Natl Acad Sci U S A. 2003;100(17):9779-84. PubMed PMID: 12902540. eng.

47. Zeng Y, Cullen BR. Sequence requirements for micro RNA processing and function in human cells. RNA. 2003 Jan;9(1):112-23. PubMed PMID: 12554881. Pubmed Central PMCID: PMC1370375. Epub 2003/01/30. eng.

48. Han J, Lee Y, Yeom KH, Nam JW, Heo I, Rhee JK, et al. Molecular basis for the recognition of primary microRNAs by the Drosha-DGCR8 complex. Cell. 2006;125(5):887-901. PubMed PMID: 16751099. eng.

49. Du T, Zamore PD. microPrimer: the biogenesis and function of microRNA. Development. 2005;132(21):4645-52. PubMed PMID: 16224044. eng.

50. Berezikov E, Chung WJ, Willis J, Cuppen E, Lai EC. Mammalian mirtron genes. Mol Cell. 2007;28(2):328-36. PubMed PMID: 17964270. eng.

51. Ruby JG, Jan CH, Bartel DP. Intronic microRNA precursors that bypass Drosha processing. Nature. 2007;448(7149):83-6. PubMed PMID: 17589500. eng.

52. Lin SL, Miller JD, Ying SY. Intronic microRNA (miRNA). J Biomed Biotechnol. 2006;2006(4):26818. PubMed PMID: 17057362. eng.

53. Zeng Y, Cullen BR. Structural requirements for pre-microRNA binding and nuclear export by Exportin 5. Nucleic Acids Res. 2004;32(16):4776-85. PubMed PMID: 15356295. eng.

54. Zhang H, Kolb FA, Brondani V, Billy E, Filipowicz W. Human Dicer preferentially cleaves dsRNAs at their termini without a requirement for ATP. EMBO J. 2002 Nov 1;21(21):5875-85. PubMed PMID: 12411505. Pubmed Central PMCID: PMC131079. Epub 2002/11/02. eng.

55. Zhang H, Kolb FA, Jaskiewicz L, Westhof E, Filipowicz W. Single processing center models for human Dicer and bacterial RNase III. Cell. 2004;118(1):57-68. PubMed PMID: 15242644. eng.

56. Song JJ, Liu J, Tolia NH, Schneiderman J, Smith SK, Martienssen RA, et al. The crystal structure of the Argonaute2 PAZ domain reveals an RNA binding motif in RNAi effector complexes. Nat Struct Biol. 2003;10(12):1026-32. PubMed PMID: 14625589. eng.

57. Brennecke J, Stark A, Russell RB, Cohen SM. Principles of microRNA-target recognition. PLoS Biol. 2005 Mar;3(3):e85. PubMed PMID: 15723116. Pubmed Central PMCID: PMC1043860. Epub 2005/02/22. eng.

58. Yekta S, Shih IH, Bartel DP. MicroRNA-directed cleavage of HOXB8 mRNA. Science. 2004;304(5670):594-6. PubMed PMID: 15105502. eng.

59. Coller J, Parker R. General translational repression by activators of mRNA decapping. Cell. 2005;122(6):875-86. PubMed PMID: 16179257. eng.

60. Meister G, Landthaler M, Patkaniowska A, Dorsett Y, Teng G, Tuschl T. Human Argonaute2 mediates RNA cleavage targeted by miRNAs and siRNAs. Mol Cell. 2004;15(2):185-97. PubMed PMID: 15260970. eng.

61. Nottrott S, Simard MJ, Richter JD. Human let-7a miRNA blocks protein production on actively translating polyribosomes. Nat Struct Mol Biol. 2006;13(12):1108-14. PubMed PMID: 17128272. eng.

62. Mallory AC, Reinhart BJ, Jones-Rhoades MW, Tang G, Zamore PD, Barton MK, et al. MicroRNA control of PHABULOSA in leaf development: importance of pairing to the microRNA 5' region. EMBO J. 2004;23(16):3356-64. PubMed PMID: 15282547. eng.

63. Mallory AC, Vaucheret H. MicroRNAs: something important between the genes. Curr Opin Plant Biol. 2004;7(2):120-5. PubMed PMID: 15003210. eng.

64. Richter D, Isono K. The mechanism of protein synthesis-initiation, elongation and termination in translation of genetic messeges. Curr Top Microbiol Immunol. 1977;76:83-125. PubMed PMID: 334484. Epub 1977/01/01. eng.

65. Petersen CP, Bordeleau ME, Pelletier J, Sharp PA. Short RNAs repress translation after initiation in mammalian cells. Mol Cell. 2006;21(4):533-42. PubMed PMID: 16483934. eng.

66. Kong YW, Cannell IG, de Moor CH, Hill K, Garside PG, Hamilton TL, et al. The mechanism of micro-RNA-mediated translation repression is determined by the promoter of the target gene. Proc Natl Acad Sci U S A. 2008;105(26):8866-71. PubMed PMID: 18579786. eng.

67. Chen CYA, Zheng D, Xia Z, Shyu AB. Ago-TNRC6 complex triggers microRNA-mediated mRNA decay by promoting biphasic deadenylation followed by decapping. Nat Struct Mol Biol. 2009 Nov;16(11):1160-6. PubMed PMID: 19838187. Pubmed Central PMCID: 2921184. eng.

68. Bartel DP. MicroRNAs: target recognition and regulatory functions. Cell. 2009 Jan 23;136(2):215-33. PubMed PMID: 19167326. Pubmed Central PMCID: Pmc3794896. Epub 2009/01/27. eng.

69. Chen CY, Zheng D, Xia Z, Shyu AB. Ago-TNRC6 triggers microRNA-mediated decay by promoting two deadenylation steps. Nat Struct Mol Biol. 2009;16(11):1160-6. PubMed PMID: 19838187. eng.

70. Hanahan D, Weinberg RA. The hallmarks of cancer. Cell. 2000;100(1):57-70. PubMed PMID: 10647931. eng.

71. Sherr CJ. Principles of tumor suppression. Cell. 2004;116(2):235-46. PubMed PMID: 14744434. eng.

72. Wu W, Sun M, Zou GM, Chen J. MicroRNA and cancer: Current status and prospective. Int J Cancer. 2007 Mar 1;120(5):953-60. PubMed PMID: 17163415. Epub 2006/12/14. eng.

73. Dalmay T, Edwards DR. MicroRNAs and the hallmarks of cancer. Oncogene. 2006;25(46):6170-5. PubMed PMID: 17028596. eng.

74. Calin GA, Liu CG, Sevignani C, Ferracin M, Felli N, Dumitru CD, et al. MicroRNA profiling reveals distinct signatures in B cell chronic lymphocytic leukemias. Proc Natl Acad Sci U S A. 2004;101(32):11755-60. PubMed PMID: 15284443. eng.

75. Lagos-Quintana M, Rauhut R, Yalcin A, Meyer J, Lendeckel W, Tuschl T. Identification of tissue-specific microRNAs from mouse. Curr Biol. 2002;12(9):735-9. PubMed PMID: 12007417. eng.

76. Calin GA, Dumitru CD, Shimizu M, Bichi R, Zupo S, Noch E, et al. Frequent deletions and down-regulation of micro- RNA genes miR15 and miR16 at 13q14 in chronic lymphocytic leukemia. Proc Natl Acad Sci U S A. 2002;99(24):15524-9. PubMed PMID: 12434020. eng.

77. Zhang B, Pan X, Cobb GP, Anderson TA. microRNAs as oncogenes and tumor suppressors. Dev Biol. 2007;302(1):1-12. PubMed PMID: 16989803. eng.

78. Jacobsen A, Silber J, Harinath G, Huse JT, Schultz N, Sander C. Analysis of microRNA-target interactions across diverse cancer types. Nature Structural & Molecular Biology. 2013 2013-10-06;20:1325-32. en.

79. Sorlie T, Tibshirani R, Parker J, Hastie T, Marron JS, Nobel A, et al. Repeated observation of breast tumor subtypes in independent gene expression data sets. Proc Natl Acad Sci U S A. 2003;100(14):8418-23. PubMed PMID: 12829800. eng.

80. Sorlie T, Perou CM, Tibshirani R, Aas T, Geisler S, Johnsen H, et al. Gene expression patterns of breast carcinomas distinguish tumor subclasses with clinical implications. Proc Natl Acad Sci U S A. 2001;98(19):10869-74. PubMed PMID: 11553815. eng.

81. Perou CM, Sorlie T, Eisen MB, van de Rijn M, Jeffrey SS, Rees CA, et al. Molecular portraits of human breast tumours. Nature. 2000 Aug 17;406(6797):747-52. PubMed PMID: 10963602. Epub 2000/08/30. eng.

82. Prat A, Parker JS, Karginova O, Fan C, Livasy C, Herschkowitz JI, et al. Phenotypic and molecular characterization of the claudin-low intrinsic subtype of breast cancer. Breast Cancer Res. 2010;12(5):R68. PubMed PMID: 20813035. eng.

83. Singh R, Mo YY. Role of microRNAs in breast cancer. Cancer Biol Ther. 2013;14(3):201-12. PubMed PMID: 23291983. eng.

84. Lund AH. miR-10 in development and cancer. Cell Death Differ. 2010;17(2):209-14. PubMed PMID: 19461655. eng.

85. Han M, Liu M, Wang Y, Mo Z, Bi X, Liu Z, et al. Re-expression of miR-21 contributes to migration and invasion by inducing epithelial-mesenchymal transition consistent with cancer stem cell characteristics in MCF-7 cells. Mol Cell Biochem. 2012 Apr;363(1-2):427-36. PubMed PMID: 22187223. Epub 2011/12/22. eng.

86. He L, Thomson JM, Hemann MT, Hernando-Monge E, Mu D, Goodson S, et al. A microRNA polycistron as a potential human oncogene. Nature. 2005;435(7043):828-33. PubMed PMID: 15944707. eng.

87. Sempere LF, Christensen M, Silahtaroglu A, Bak M, Heath CV, Schwartz G, et al. Altered MicroRNA expression confined to specific epithelial cell subpopulations in breast cancer. Cancer Res. 2007;67(24):11612-20. PubMed PMID: 18089790. eng.

88. Korpal M, Lee ES, Hu G, Kang Y. The miR-200 family inhibits epithelial-mesenchymal transition and cancer cell migration by direct targeting of E-cadherin transcriptional repressors ZEB1 and ZEB2. J Biol Chem. 2008;283(22):14910-4. PubMed PMID: 18411277. eng.

89. Akhavantabasi S, Sapmaz A, Tuna S, Erson-Bensan AE. miR-125b targets ARID3B in breast cancer cells. Cell Struct Funct. 2012;37(1):27-38. PubMed PMID: 22307404. eng.

90. Akman HB, Selcuklu SD, Donoghue MT, Akhavantabasi S, Sapmaz A, Spillane C, et al. ALCAM is indirectly modulated by miR-125b in MCF7 cells. Tumour Biol. 2014 Dec 25. PubMed PMID: 25539763. Epub 2014/12/30. Eng.

91. Feliciano A, Castellvi J, Artero-Castro A, Leal JA, Romagosa C, Hernandez-Losa J, et al. miR-125b acts as a tumor suppressor in breast tumorigenesis via its novel direct targets ENPEP, CK2-alpha, CCNJ, and MEGF9. PLoS One. 2013;8(10):e76247. PubMed PMID: 24098452. eng.

92. Xie B, Ding Q, Han H, Wu D. miRCancer: a microRNA-cancer association database constructed by text mining on literature. Bioinformatics. 2013;29(5):638-44. PubMed PMID: 23325619. eng.

93. Abbott AL. Uncovering new functions for microRNAs in Caenorhabditis elegans. Curr Biol. 2011;21(17):R668-71. PubMed PMID: 21920301. eng.

94. Wightman B, Ha I, Ruvkun G. Posttranscriptional regulation of the heterochronic gene lin-14 by lin-4 mediates temporal pattern formation in C. elegans. Cell. 1993;75(5):855-62. PubMed PMID: 8252622. eng.

95. Calin GA, Sevignani C, Dumitru CD, Hyslop T, Noch E, Yendamuri S, et al. Human microRNA genes are frequently located at fragile sites and genomic regions involved in cancers. Proc Natl Acad Sci U S A. 2004;101(9):2999-3004. PubMed PMID: 14973191. eng.

96. Shang C, Lu YM, Meng LR. MicroRNA-125b down-regulation mediates endometrial cancer invasion by targeting ERBB2. Med Sci Monit. 2012;18(4):BR149-55. PubMed PMID: 22460089. eng.

97. Smits M, Wurdinger T, van het Hof B, Drexhage JA, Geerts D, Wesseling P, et al. Myc-associated zinc finger protein (MAZ) is regulated by miR-125b and mediates VEGF-induced angiogenesis in glioblastoma. FASEB J. 2012;26(6):2639-47. PubMed PMID: 22415301. eng.

98. Liu LH, Li H, Li JP, Zhong H, Zhang HC, Chen J, et al. miR-125b suppresses the proliferation and migration of osteosarcoma cells through down-regulation of STAT3. Biochem Biophys Res Commun. 2011;416(1-2):31-8. PubMed PMID: 22093834. eng.

99. Nakanishi H, Taccioli C, Palatini J, Fernandez-Cymering C, Cui R, Kim T, et al. Loss of miR-125b-1 contributes to head and neck cancer development by dysregulating TACSTD2 and MAPK pathway. Oncogene. 2014;33(6):702-12. PubMed PMID: 23416980. eng.

100. Zhang Y, Yan LX, Wu QN, Du ZM, Chen J, Liao DZ, et al. miR-125b is methylated and functions as a tumor suppressor by regulating the ETS1 proto-oncogene in human invasive breast cancer. Cancer Res. 2011;71(10):3552-62. PubMed PMID: 21444677. eng.

101. He J, Xu Q, Jing Y, Agani F, Qian X, Carpenter R, et al. Reactive oxygen species regulate ERBB2 and ERBB3 expression via miR-199a/125b and DNA methylation. EMBO Rep. 2012;13(12):1116-22. PubMed PMID: 23146892. eng.

102. Banzhaf-Strathmann J, Edbauer D. Good guy or bad guy: the opposing roles of microRNA 125b in cancer. Cell Commun Signal. 2014;12:30. PubMed PMID: 24774301. eng.

103. Lee YS, Kim HK, Chung S, Kim KS, Dutta A. Depletion of human micro-RNA miR-125b reveals that it is critical for the proliferation of differentiated cells but not for the down-regulation of putative targets during differentiation. J Biol Chem. 2005;280(17):16635-41. PubMed PMID: 15722555. eng.

104. Le MT, Shyh-Chang N, Khaw SL, Chin L, Teh C, Tay J, et al. Conserved regulation of p53 network dosage by microRNA-125b occurs through evolving miRNA-target gene pairs. PLoS Genet. 2011;7(9):e1002242. PubMed PMID: 21935352. eng.

105. Muller PA, Vousden KH. p53 mutations in cancer. Nat Cell Biol. 2013;15(1):2-8. PubMed PMID: 23263379. eng.

106. Le MT, Teh C, Shyh-Chang N, Xie H, Zhou B, Korzh V, et al. MicroRNA-125b is a novel negative regulator of p53. Genes Dev. 2009;23(7):862-76. PubMed PMID: 19293287. eng.

107. Yarden Y. Biology of HER2 and its importance in breast cancer. Oncology. 2001;61 Suppl 2:1-13. PubMed PMID: 11694782. eng.

108. Tan M, Yu D. Molecular mechanisms of erbB2-mediated breast cancer chemoresistance. Adv Exp Med Biol. 2007;608:119-29. PubMed PMID: 17993237. Epub 2007/11/13. eng.

109. Canfield K, Li J, Wilkins OM, Morrison MM, Ung M, Wells W, et al. Receptor tyrosine kinase ERBB4 mediates acquired resistance to ERBB2 inhibitors in breast cancer cells. Cell Cycle. 2015;14(4):648-55. PubMed PMID: 25590338. Epub 2015/01/16. eng.

110. Scott GK, Goga A, Bhaumik D, Berger CE, Sullivan CS, Benz CC. Coordinate suppression of ERBB2 and ERBB3 by enforced expression of micro-RNA miR-125a or miR-125b. J Biol Chem. 2007;282(2):1479-86. PubMed PMID: 17110380. eng.

111. Mattie MD, Benz CC, Bowers J, Sensinger K, Wong L, Scott GK, et al. Optimized high-throughput microRNA expression profiling provides novel biomarker assessment of clinical prostate and breast cancer biopsies. Mol Cancer. 2006;5:24. PubMed PMID: 16784538. eng.

112. Microarray analysis of PDGFRα+ populations in ES cell differentiation culture identifies genes involved in differentiation of mesoderm and mesenchyme including ARID3b that is essential for development of embryonic mesenchymal cells. 2006 1 May 2006;293(1):25–37.

113. Kobayashi K, Era T, Takebe A, Jakt LM, Nishikawa S-I. ARID3B Induces Malignant Transformation of Mouse Embryonic Fibroblasts and Is Strongly Associated with Malignant Neuroblastoma. 2006 2006-09-01. en.

114. PLOS ONE: ARID3B Induces Tumor Necrosis Factor Alpha Mediated Apoptosis While a Novel ARID3B Splice Form Does Not Induce Cell Death. 2015.

115. Ferracin M, Bassi C, Pedriali M, Pagotto S, D'Abundo L, Zagatti B, et al. miR-125b targets erythropoietin and its receptor and their expression correlates with metastatic potential and ERBB2/HER2 expression. Mol Cancer. 2013;12(1):130. PubMed PMID: 24165569. eng.

116. Huang L, Department of Urology SYsMH, Sun Yat-sen University, Guangzhou, China, Luo J, Department of Urology SYsMH, Sun Yat-sen University, Guangzhou, China, Cai Q, Department of Internal Medicine CC, Sun Yat-sen University, Guangzhou, China, et al. MicroRNA-125b suppresses the development of bladder cancer by targeting E2F3. International Journal of Cancer. 2015;128(8):1758-69. en.

117. Guan Y, Department of Medical Genetics CMU, Shenyang, China, Yao H, Laboratory of Neural Signal Transduction IoN, Shanghai Institute for Biological Sciences, State Key Laboratory of Neuroscience, Shanghai, China, Zheng Z, Department of Medical Genetics CMU, Shenyang, China, et al. MiR-125b targets BCL3 and suppresses ovarian cancer proliferation. International Journal of Cancer. 2015;128(10):2274-83. en.

118. Svoboda M, Izakovicova Holla L, Sefr R, Vrtkova I, Kocakova I, Tichy B, et al. Micro-RNAs miR125b and miR137 are frequently upregulated in response to capecitabine chemoradiotherapy of rectal cancer. Int J Oncol. 2008 Sep;33(3):541-7. PubMed PMID: 18695884. Epub 2008/08/13. eng.

119. Xia HF, He TZ, Liu CM, Cui Y, Song PP, Jin XH, et al. MiR-125b expression affects the proliferation and apoptosis of human glioma cells by targeting Bmf. Cell Physiol Biochem. 2009;23(4-6):347-58. PubMed PMID: 19471102. eng.

120. Bloomston M, Frankel WL, Petrocca F, Volinia S, Alder H, Hagan JP, et al. MicroRNA expression patterns to differentiate pancreatic adenocarcinoma from normal pancreas and chronic pancreatitis. JAMA. 2007;297(17):1901-8. PubMed PMID: 17473300. eng.

121. Li X, Zhang Y, Zhang H, Liu X, Gong T, Li M, et al. miRNA-223 promotes gastric cancer invasion and metastasis by targeting tumor suppressor EPB41L3. Mol Cancer Res. 2011;9(7):824-33. PubMed PMID: 21628394. eng.

122. Vriens MR, Weng J, Suh I, Huynh N, Guerrero MA, Shen WT, et al. MicroRNA expression profiling is a potential diagnostic tool for thyroid cancer. Cancer. 2012 Jul 1;118(13):3426-32. PubMed PMID: 22006248. Epub 2011/10/19. eng.

123. Bousquet M, Harris MH, Zhou B, Lodish HF. MicroRNA miR-125b causes leukemia. Proc Natl Acad Sci U S A. 2010;107(50):21558-63. PubMed PMID: 21118985. eng.

124. Iorio MV, Visone R, Di Leva G, Donati V, Petrocca F, Casalini P, et al. MicroRNA signatures in human ovarian cancer. Cancer Res. 2007;67(18):8699-707. PubMed PMID: 17875710. eng.

125. Zhou Y, Eppenberger-Castori S, Eppenberger U, Benz CC. The NFkappaB pathway and endocrine-resistant breast cancer. Endocr Relat Cancer. 2005 Jul;12 Suppl 1:S37-46. PubMed PMID: 16113098. Epub 2005/08/23. eng.

126. Karin M. How NF-kappaB is activated: the role of the IkappaB kinase (IKK) complex. Oncogene. 1999 Nov 22;18(49):6867-74. PubMed PMID: 10602462. Epub 1999/12/22. eng.

127. Ko BS, Chang TC, Chen CH, Liu CC, Kuo CC, Hsu C, et al. Bortezomib suppresses focal adhesion kinase expression via interrupting nuclear factor-kappa B. Life Sci. 2010 Jan 30;86(5-6):199-206. PubMed PMID: 20006625. Epub 2009/12/17. eng.

128. Kendellen MF, Bradford JW, Lawrence CL, Clark KS, Baldwin AS. Canonical and non-canonical NF-kappaB signaling promotes breast cancer tumor-initiating cells. Oncogene. 2014 Mar 6;33(10):1297-305. PubMed PMID: 23474754. Pubmed Central PMCID: Pmc4425414. Epub 2013/03/12. eng.

129. Michel M, Wilhelmi I, Schultz AS, Preussner M, Heyd F. Activation-induced tumor necrosis factor receptor-associated factor 3 (Traf3) alternative splicing controls the noncanonical nuclear factor kappaB pathway and chemokine expression in human T cells. J Biol Chem. 2014 May 9;289(19):13651-60. PubMed PMID: 24671418. Pubmed Central PMCID: Pmc4036369. Epub 2014/03/29. eng.

130. Wu Y, Deng J, Rychahou PG, Qiu S, Evers BM, Zhou BP. Stabilization of snail by NF-kappaB is required for inflammation-induced cell migration and invasion. Cancer Cell. 2009 May 5;15(5):416-28. PubMed PMID: 19411070. Pubmed Central PMCID: Pmc2881229. Epub 2009/05/05. eng.

131. Shostak K, Chariot A. NF-κB, stem cells and breast cancer: the links get stronger. Breast Cancer Research. 2011 2011-07-26;13(4):214. en.

132. Biswas DK, Cruz AP, Gansberger E, Pardee AB. Epidermal growth factor-induced nuclear factor κB activation: A major pathway of cell-cycle progression in estrogen-receptor negative breast cancer cells. Proc Natl Acad Sci U S A. 2000;97(15):8542-7. PubMed PMID: 10900013. eng.

133. Van Laere SJ, Van der Auwera I, Van den Eynden GG, van Dam P, Van Marck EA, Vermeulen PB, et al. NF-kappaB activation in inflammatory breast cancer is associated with oestrogen receptor downregulation, secondary to EGFR and/or ErbB2 overexpression and MAPK hyperactivation. Br J Cancer. 2007 Sep 3;97(5):659-69. PubMed PMID: 17700572. Pubmed Central PMCID: Pmc2360371. Epub 2007/08/19. eng.

134. Qiu J, Wang X, Guo X, Zhao C, Wu X, Zhang Y. Toll-like receptor 9 agonist inhibits ERalpha-mediated transactivation by activating NF-kappaB in breast cancer cell lines. Oncol Rep. 2009 Oct;22(4):935-41. PubMed PMID: 19724876. Epub 2009/09/03. eng.

135. Paimela T, Ryhanen T, Mannermaa E, Ojala J, Kalesnykas G, Salminen A, et al. The effect of 17beta-estradiol on IL-6 secretion and NF-kappaB DNA-binding activity in human retinal pigment epithelial cells. Immunol Lett. 2007 Jun 15;110(2):139-44. PubMed PMID: 17532054. Epub 2007/05/29. eng.

136. Galien R, Garcia T. Estrogen receptor impairs interleukin-6 expression by preventing protein binding on the NF-kappaB site. Nucleic Acids Res. 1997 Jun 15;25(12):2424-9. PubMed PMID: 9171095. Pubmed Central PMCID: Pmc146754. Epub 1997/06/15. eng.

137. Hsu SM, Chen YC, Jiang MC. 17 beta-estradiol inhibits tumor necrosis factor-alpha-induced nuclear factor-kappa B activation by increasing nuclear factor-kappa B p105 level in MCF-7 breast cancer cells. Biochem Biophys Res Commun. 2000 Dec 9;279(1):47-52. PubMed PMID: 11112416. Epub 2000/12/09. eng.

138. Nettles KW, Gil G, Nowak J, Metivier R, Sharma VB, Greene GL. CBP Is a dosage-dependent regulator of nuclear factor-kappaB suppression by the estrogen receptor. Mol Endocrinol. 2008 Feb;22(2):263-72. PubMed PMID: 17932106. Pubmed Central PMCID: Pmc2234588. Epub 2007/10/13. eng.

139. Sas L, Lardon F, Vermeulen PB, Hauspy J, Van Dam P, Pauwels P, et al. The interaction between ER and NFκB in resistance to endocrine therapy. Breast Cancer Research. 2012 2012-08-31;14(4):212. en.

140. Frasor J, Weaver A, Pradhan M, Dai Y, Miller LD, Lin CY, et al. Positive cross-talk between estrogen receptor and NF-kappaB in breast cancer. Cancer Res. 2009 Dec 1;69(23):8918-25. PubMed PMID: 19920189. Pubmed Central PMCID: Pmc2996265. Epub 2009/11/19. eng.

141. Sas L, Lardon F, Vermeulen PB, Hauspy J, Van Dam P, Pauwels P, et al. The interaction between ER and NFkappaB in resistance to endocrine therapy. Breast Cancer Res. 2012;14(4):212. PubMed PMID: 22963717. Pubmed Central PMCID: Pmc3680926. Epub 2012/09/12. eng.

142. Pradhan M, Bembinster LA, Baumgarten SC, Frasor J. Proinflammatory cytokines enhance estrogen-dependent expression of the multidrug transporter gene ABCG2 through estrogen receptor and NF{kappa}B cooperativity at adjacent response elements. J Biol Chem. 2010 Oct 8;285(41):31100-6. PubMed PMID: 20705611. Pubmed Central PMCID: Pmc2951183. Epub 2010/08/14. eng.

143. Rubio MF, Werbajh S, Cafferata EG, Quaglino A, Colo GP, Nojek IM, et al. TNF-alpha enhances estrogen-induced cell proliferation of estrogen-dependent breast tumor cells through a complex containing nuclear factor-kappa B. Oncogene. 2006 Mar 2;25(9):1367-77. PubMed PMID: 16331275. Epub 2005/12/07. eng.

144. Kim MR, Choi HK, Cho KB, Kim HS, Kang KW. Involvement of Pin1 induction in epithelial-mesenchymal transition of tamoxifen-resistant breast cancer cells. Cancer Sci. 2009 Oct;100(10):1834-41. PubMed PMID: 19681904. Epub 2009/08/18. eng.

145. Li T, Morgan MJ, Choksi S, Zhang Y, Kim YS, Liu ZG. MicroRNAs modulate the noncanonical transcription factor NF-kappaB pathway by regulating expression of the kinase IKKalpha during macrophage differentiation. Nat Immunol. 2010 Sep;11(9):799-805. PubMed PMID: 20711193. Pubmed Central PMCID: Pmc2926307. Epub 2010/08/17. eng.

146. Zhou R, Hu G, Liu J, Gong AY, Drescher KM, Chen XM. NF-kappaB p65-dependent transactivation of miRNA genes following Cryptosporidium parvum infection stimulates epithelial cell immune responses. PLoS Pathog. 2009 Dec;5(12):e1000681. PubMed PMID: 19997496. Pubmed Central PMCID: Pmc2778997. Epub 2009/12/10. eng.

147. Kim SW, Ramasamy K, Bouamar H, Lin AP, Jiang D, Aguiar RC. MicroRNAs miR-125a and miR-125b constitutively activate the NF-kappaB pathway by targeting the tumor necrosis factor alpha-induced protein 3 (TNFAIP3, A20). Proc Natl Acad Sci U S A. 2012 May 15;109(20):7865-70. PubMed PMID: 22550173. Pubmed Central PMCID: Pmc3356650. Epub 2012/05/03. eng.

148. Haemmig S, Baumgartner U, Gluck A, Zbinden S, Tschan MP, Kappeler A, et al. miR-125b controls apoptosis and temozolomide resistance by targeting TNFAIP3 and NKIRAS2 in glioblastomas. Cell Death Dis. 2014;5:e1279. PubMed PMID: 24901050. Epub 2014/06/06. eng.

149. Ngo VN, Young RM, Schmitz R, Jhavar S, Xiao W, Lim KH, et al. Oncogenically active MYD88 mutations in human lymphoma. Nature. 2011 Feb 3;470(7332):115-9. PubMed PMID: 21179087. Epub 2010/12/24. eng.

150. Pasqualucci L, Trifonov V, Fabbri G, Ma J, Rossi D, Chiarenza A, et al. Analysis of the coding genome of diffuse large B-cell lymphoma. Nat Genet. 2011 Sep;43(9):830-7. PubMed PMID: 21804550. Pubmed Central PMCID: Pmc3297422. Epub 2011/08/02. eng.

151. Westerheide SD, Mayo MW, Anest V, Hanson JL, Baldwin AS. The Putative Oncoprotein Bcl-3 Induces Cyclin D1 To Stimulate G1 Transition. Mol Cell Biol. 2001;21(24):8428-36. PubMed PMID: 11713278. eng.

152. Huang K, Dong S, Li W, Xie Z. The expression and regulation of microRNA-125b in cancers. 2013 2013-06-25. en.

153. Wang X, Ha T, Zou J, Ren D, Liu L, Zhang X, et al. MicroRNA-125b protects against myocardial ischaemia/reperfusion injury via targeting p53-mediated apoptotic signalling and TRAF6. Cardiovasc Res. 2014 Jun 1;102(3):385-95. PubMed PMID: 24576954. Pubmed Central PMCID: Pmc4030511. Epub 2014/03/01. eng.

154. Wang X, Ha T, Zou J, Ren D, Liu L, Zhang X, et al. MicroRNA-125b protects against myocardial ischaemia/reperfusion injury via targeting p53-mediated apoptotic signalling and TRAF6. 2014 2014-06-01. en.

155. Suzuki HI, Miyazono K. Emerging complexity of microRNA generation cascades. J Biochem. 2011 Jan;149(1):15-25. PubMed PMID: 20876186. Epub 2010/09/30. eng.

156. Fukuda T, Yamagata K, Fujiyama S, Matsumoto T, Koshida I, Yoshimura K, et al. DEAD-box RNA helicase subunits of the Drosha complex are required for processing of rRNA and a subset of microRNAs. Nat Cell Biol. 2007 May;9(5):604-11. PubMed PMID: 17435748. Epub 2007/04/17. eng.

157. Qin W, Shi Y, Zhao B, Yao C, Jin L, Ma J, et al. miR-24 regulates apoptosis by targeting the open reading frame (ORF) region of FAF1 in cancer cells. PLoS One. 2010;5(2):e9429. PubMed PMID: 20195546. Pubmed Central PMCID: Pmc2828487. Epub 2010/03/03. eng.

158. Yamagata K, Fujiyama S, Ito S, Ueda T, Murata T, Naitou M, et al. RETRACTED: Maturation of MicroRNA Is Hormonally Regulated by a Nuclear Receptor. Molecular Cell. 2015;36(2):340-7.

159. Paris O, Ferraro L, Grober OM, Ravo M, De Filippo MR, Giurato G, et al. Direct regulation of microRNA biogenesis and expression by estrogen receptor beta in hormone-responsive breast cancer. Oncogene. 2012 Sep 20;31(38):4196-206. PubMed PMID: 22231442. Epub 2012/01/11. eng.

160. Paroo Z, Ye X, Chen S, Liu Q. Phosphorylation of the human microRNA-generating complex mediates MAPK/Erk signaling. Cell. 2009 Oct 2;139(1):112-22. PubMed PMID: 19804757. Pubmed Central PMCID: Pmc2760040. Epub 2009/10/07. eng.

161. Levin ER. Minireview: Extranuclear steroid receptors: roles in modulation of cell functions. Mol Endocrinol. 2011 Mar;25(3):377-84. PubMed PMID: 20861220. Pubmed Central PMCID: Pmc3045744. Epub 2010/09/24. eng.

162. Bhat-Nakshatri P, Wang G, Collins NR, Thomson MJ, Geistlinger TR, Carroll JS, et al. Estradiol-regulated microRNAs control estradiol response in breast cancer cells. Nucleic Acids Res. 2009 Aug;37(14):4850-61. PubMed PMID: 19528081. Pubmed Central PMCID: Pmc2724297. Epub 2009/06/17. eng.

163. Adams BD, Claffey KP, White BA. Argonaute-2 expression is regulated by epidermal growth factor receptor and mitogen-activated protein kinase signaling and correlates with a transformed phenotype in breast cancer cells. Endocrinology. 2009 Jan;150(1):14-23. PubMed PMID: 18787018. Pubmed Central PMCID: Pmc2630894. Epub 2008/09/13. eng.

164. Klinge CM. miRNAs and estrogen action. Trends Endocrinol Metab. 2012 May;23(5):223-33. PubMed PMID: 22503553. Pubmed Central PMCID: Pmc3348384. Epub 2012/04/17. eng.

165. Bailey ST, Westerling T, Brown M. Loss of estrogen-regulated microRNA expression increases HER2 signaling and is prognostic of poor outcome in luminal breast cancer. Cancer Res. 2015 Jan 15;75(2):436-45. PubMed PMID: 25388283. Pubmed Central PMCID: Pmc4297564. Epub 2014/11/13. eng.

166. Chen PY, Manninga H, Slanchev K, Chien M, Russo JJ, Ju J, et al. The developmental miRNA profiles of zebrafish as determined by small RNA cloning. Genes Dev. 2005;19(11):1288-93. PubMed PMID: 15937218. eng.

167. Laganiere J, Deblois G, Lefebvre C, Bataille AR, Robert F, Giguere V. From the Cover: Location analysis of estrogen receptor alpha target promoters reveals that FOXA1 defines a domain of the estrogen response. Proc Natl Acad Sci U S A. 2005 Aug 16;102(33):11651-6. PubMed PMID: 16087863. Pubmed Central PMCID: Pmc1183449. Epub 2005/08/10. eng.

168. Wang J, Gu Z, Ni P, Qiao Y, Chen C, Liu X, et al. NF-kappaB P50/P65 hetero-dimer mediates differential regulation of CD166/ALCAM expression via interaction with micoRNA-9 after serum deprivation, providing evidence for a novel negative auto-regulatory loop. Nucleic Acids Res. 2011;39(15):6440-55. PubMed PMID: 21572107. eng.

169. Maguire O, Collins C, O'Loughlin K, Miecznikowski J, Minderman H. Quantifying nuclear p65 as a parameter for NF-kappaB activation: Correlation between ImageStream cytometry, microscopy, and Western blot. Cytometry A. 2011 Jun;79(6):461-9. PubMed PMID: 21520400. Pubmed Central PMCID: Pmc3140714. Epub 2011/04/27. eng.

170. Dickson KM, Bhakar AL, Barker PA. TRAF6-dependent NF-kB transcriptional activity during mouse development. Dev Dyn. 2004 Sep;231(1):122-7. PubMed PMID: 15305292. Epub 2004/08/12. eng.

APPENDIX A

MAMMALIAN CELL CULTURE PEROPERTIES

Below table shows the basic properties of breast cancer cell lines which were used in this study. These properties include source of tumor, tumor type and tumor subtype and ER-PR-ERBB2 gene status.

Table A.1. Mammalian cell lines' properties.

Cell Lines	Subtypes	ER Status	PR Status	ERBB2 Status	Source	Tumor type
MCF7	Luminal	+	+	-	Pleural Effusion	Metastatic Adenocarcinoma
T47D	Luminal	+	+	-	Pleural Effusion	Invasive Ductal Carcinoma

APPENDIX B

RNA QUANTIFICATION, DNA CONTAMINITATION AND cDNA SYNTHESIS CONFIRMATION

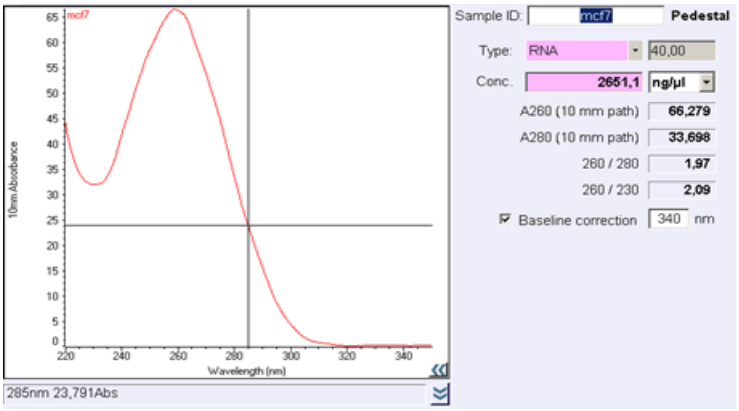

Figure B.1.: RNA concentrations were determined using NanoDrop ND1000 (Thermo Scientific). Purity was determined by A260/A280 and A260/A230 ratios.

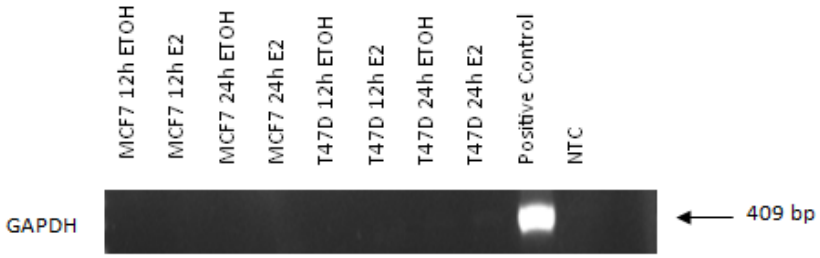

Figure B.2.: Confirmation of lack of DNA contamination in RNA samples. PCR was performed using GAPDH specific primers. GAPDH_F: 5'-GGGAGCCAAAAGGGTCATCA3' and GAPDH_R: 5'-TTTCTAGACGGCAGGTCA GGT-3' (product size: 409 bp). Following conditions were used for the PCR reactions: incubation at 94°C for 10 minutes, 40 cycles of 94°C for 30 seconds, 56°C for 30 seconds, and 72°C for 30 seconds, and final extension at 72°C for 5 minutes. Genomic DNA was used as a positive control.

APPENDIX C

TAQMAN QPCR ASSAY PERFORMANCE RESULTS

U6 TaqMan- qPCR Assay Performance Results

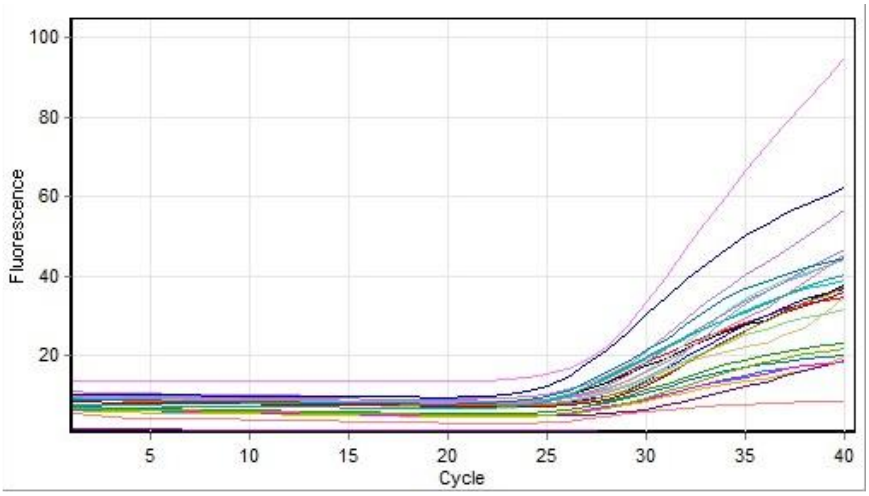

Figure C.1. Raw Data For Cycling A.Green

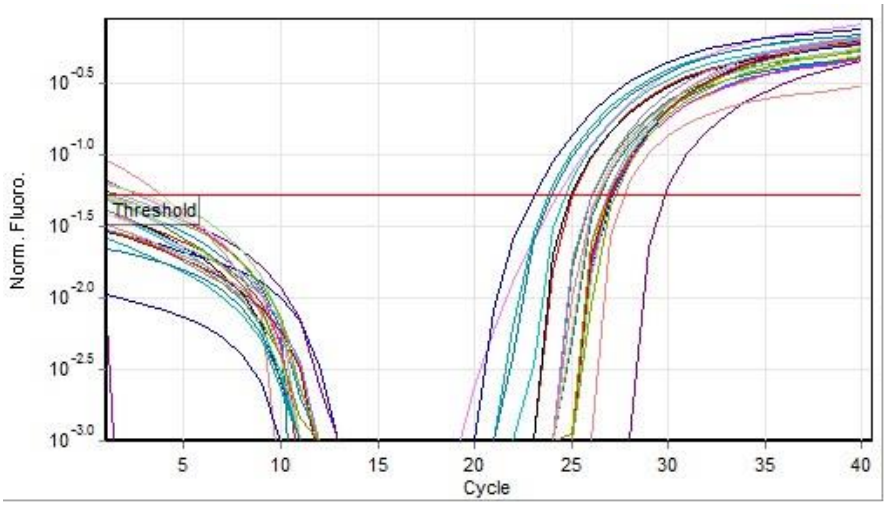

Figure C.2. Quantitation data for Cycling A.Green

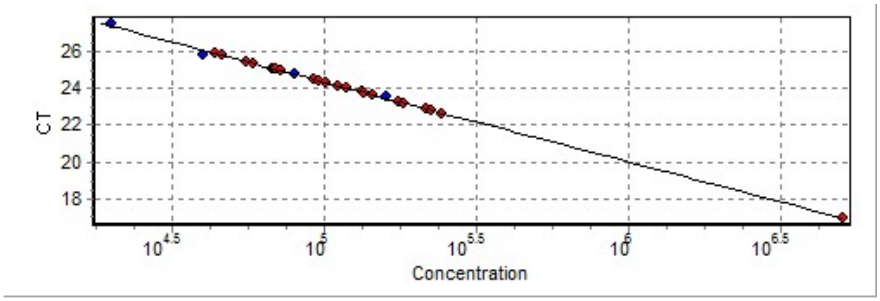

Figure C.3. Standard Curve

No.	Colour	Name	Type	Ct	Given Conc (copies/reaction)	Calc Conc (copies/reaction)	% Var
1		no dil: U6	Standard	23.51	160,000	153,727	3.9%
2		1:2	Standard	24.72	80,000	80,290	0.4%
3		1:4	Standard	25.82	40,000	44,774	11.9%
4		1:8	Standard	27.47	20,000	18,530	7.4%
26		NTC	NTC				

Figure C4. qRT-PCR assay performance shown with respect to MIQE guidelines. Raw fluoresence data, quantitation data, standard curve and quantitation information was analyzed by RotorGene Software for RNU6B primers. In TaqMan probe systems melting curve analysis is not performed.

Threshold	0,1232
Left Threshold	1,000
Standard Curve Imported	No
Standard Curve (1)	conc= 10^(-0,311*CT + 12,108)
Standard Curve (2)	CT = -3,215*log(conc) + 38,925
Reaction efficiency (*)	1,04669 (* = 10^(-1/m) - 1)
M	-3,21489
B	38,92467
R Value	0,99972
R^2 Value	0,99945
Start normalising from cycle	1
Noise Slope Correction	No
No Template Control Threshold	0%
Reaction Efficiency Threshold	Disabled
Normalisation Method	Dynamic Tube Normalisation
Digital Filter	Light
Sample Page	Page 1
Imported Analysis Settings	

Figure C.5. Quantitation Information. qRT-PCR assay performance shown with respect to MIQE guidelines. Raw fluoresence data, quantitation data, standard curve and quantitation information was analyzed by RotorGene Software for RNU6B primers. In TaqMan probe systems melting curve analysis is not performed.

miR-125b TaqMan- qPCR Assay Performance Results

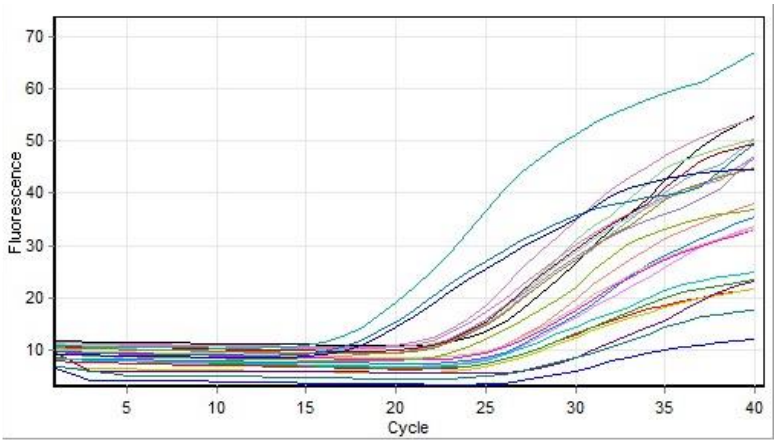

Figure C.6. Raw Data For Cycling A.Green

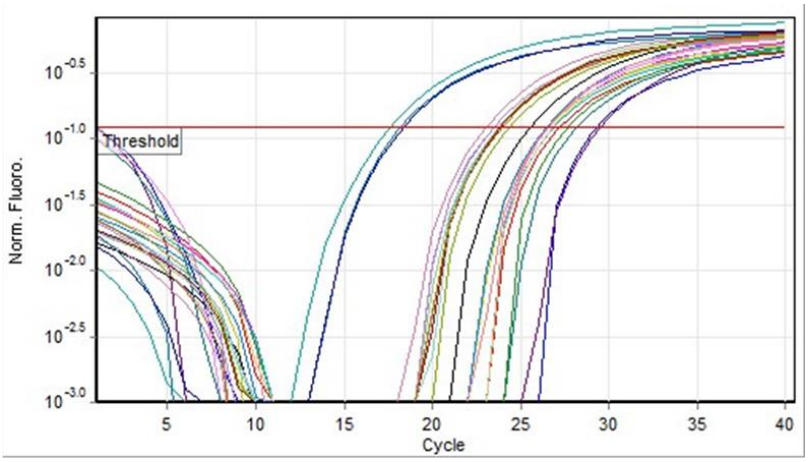

Figure C.7. Quantitation data for Cycling A.Green

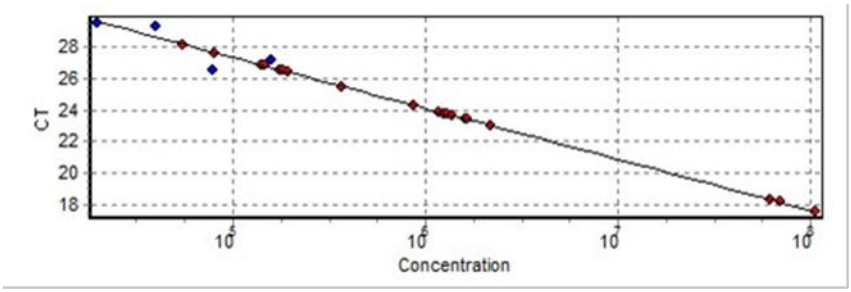

Figure C.8. Standard Curve

No.	Colour	Name	Type	Ct	Given Conc (copies/reaction)	Calc Conc (copies/reaction)	% Var
1		no dil 125b	Standard	27.17	160,000	158,701	3.2%
2		1:2	Standard	26.54	80,000	75,458	9.3%
3		1:4	Standard	29.30	40,000	37,439	3.9%
4		1:8	Standard	29.49	20,000	21,379	6.9%
26		NTC	NTC				

Figure C9. qRT-PCR assay performance shown with respect to MIQE guidelines. Raw fluoresence data, quantitation data, standard curve and quantitation information was analyzed by RotorGene Software for miR-125b primers. In TaqMan probe systems melting curve analysis is not performed.

Threshold	0.1221
Left Threshold	1.000
Standard Curve Imported	No
Standard Curve (1)	conc= 10^(-0.310*CT + 13.470)
Standard Curve (2)	CT = -3.226*log(conc) + 43.457
Reaction efficiency (*)	1.04153 (* = 10^(-1/m) - 1)
M	-3.22628
B	43.45682
R Value	0.84113
R^2 Value	0.70751
Start normalising from cycle	1
Noise Slope Correction	No
No Template Control Threshold	0%
Reaction Efficiency Threshold	Disabled
Normalisation Method	Dynamic Tube Normalisation
Digital Filter	Light
Sample Page	Page 1
Imported Analysis Settings	

Figure C.10. Quantitation Information. qRT-PCR assay performance shown with respect to MIQE guidelines. Raw fluoresence data, quantitation data, standard curve and quantitation information was analyzed by RotorGene Software for miR-125b primers. In TaqMan probe systems melting curve analysis is not performed.

miR-125a TaqMan- qPCR Assay Performance Results

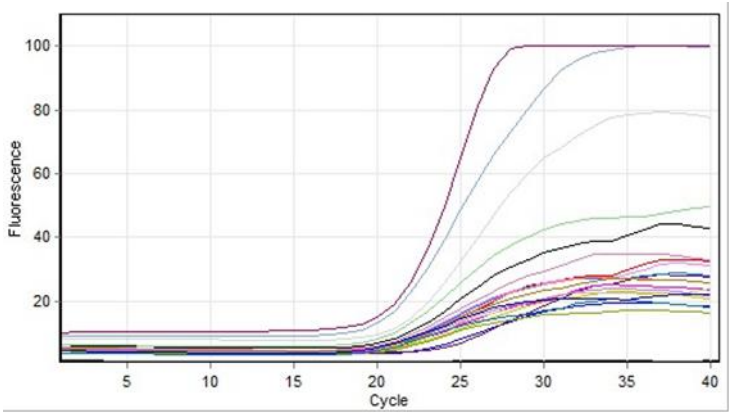

Figure C.11. Raw Data For Cycling A.Green

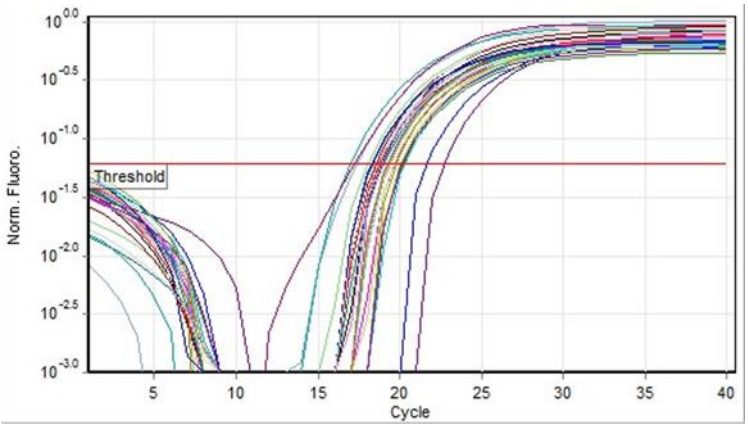

Figure C.12. Quantitation data for Cycling A.Green

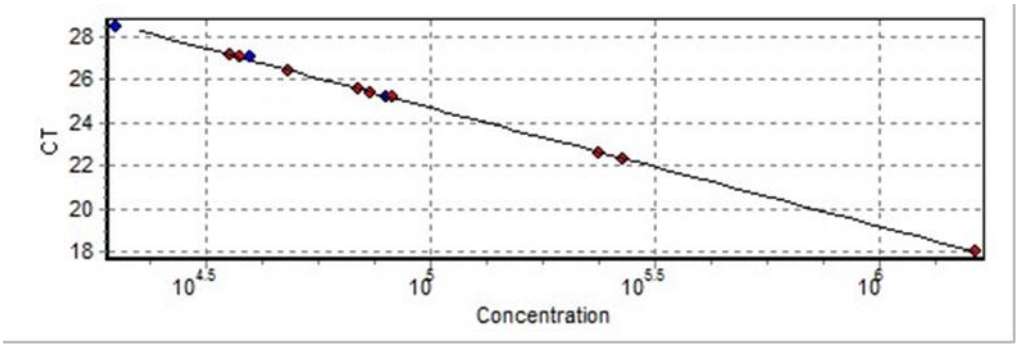

Figure C.13. Standard Curve

No.	Colour	Name	Type	Ct	Given Conc (copies/ul)	Calc Conc (copies/ul)	% Var
1		no dil:	Standard	27.82	160,000	145,797	8.9%
2		1:2	Standard	28.67	80,000	83,428	6.8%
3		1:4	Standard	30.35	40,000	38,761	3.1%
4		1:8	Standard	31.68	20,000	19,394	3.0%
29		NTC	NTC				

Figure C.14. qRT-PCR assay performance shown with respect to MIQE guidelines. Raw fluoresence data, quantitation data, standard curve and quantitation information was analyzed by RotorGene Software for miR-125a primers. In TaqMan probe systems melting curve analysis is not performed.

Threshold	0.0612
Left Threshold	1.000
Standard Curve Imported	No
Standard Curve (1)	conc= 10^(-0.227*CT + 9.463)
Standard Curve (2)	CT = -4.411*log(conc) + 41.743
Reaction efficiency (*)	0.98539 (* = 10^(-1/m) - 1)
M	-4.41111
B	41.74295
R Value	0.9972
R^2 Value	0.99441
Start normalising from cycle	1
Noise Slope Correction	No
No Template Control Threshold	0%
Reaction Efficiency Threshold	Disabled
Normalisation Method	Dynamic Tube Normalisation
Digital Filter	Light
Sample Page	Page 1
Imported Analysis Settings	

Fİgure C.12. Quantitation Information. qRT-PCR assay performance shown with respect to MIQE guidelines. Raw fluoresence data, quantitation data, standard curve and quantitation information was analyzed by RotorGene Software for miR-125a primers. In TaqMan probe systems melting curve analysis is not performed.

APPENDIX D

MARKERS

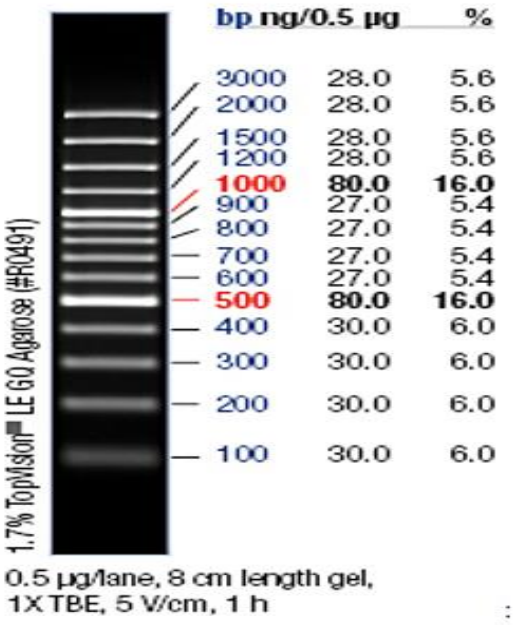

Figure D.1.: GeneRuler 100 bp DNA Ladder Plus.

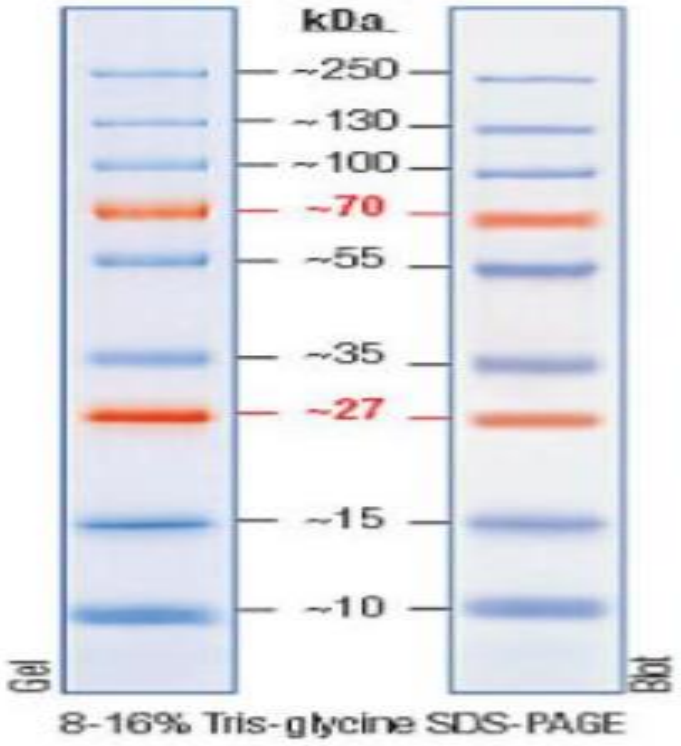

Figure D.2.: PageRuler Pre-stained Protein Ladder. Fermentas SM1811 Protein ladder was used during Western Blot experiments.

APPENDIX E

BUFFERS

TBS-T:

20 mM Tris

137 mM NaCl

0.1% Tween 20

pH: 7.6

PBS-T:

137mM NaCl

2,7mM KCl

10mM Na_2HPO_4.2H2O

2mM KH_2PO_4

0.1% Tween 20

pH: 7.4

6X Laemmli Buffer:

12% SDS

30% 2-mercaptoethanol

60% Glycerol

0.012% bromophenol blue

0.375 M Tris

APPENDIX F

CHARCOAL DEXTRAN TREATMENT OF FETAL BOVINE SERUM

For 500 ml of fetal bovine serum (FBS), 10 g of charcoal, dextran coated from Sigma (Product#C6241) is added. 250 ml FBS and 5 g dextran coated charcoal are added to two 500 ml centrifuge bottles (Nalgene, polycarbonate, autoclaved). This mixture is incubated for overnight at 4°C with agitation (by using a shaker at 100 rpm, or similar). Charcoal is precipitated by centrifuging at 10800xg for 30 minutes at 4°C. In a biological safety cabinet, supernatant is tranfered carefully into new 500 ml centrifuge bottles. Remaining charcoal is precipitated by centrifuging at 10800xg for 30 minutes at 4°C. Supernatant is transferred into new 500 ml centrifuge bottles. 5 g of dextran coated charcoal is added again to this remaining supernatant. Mixture is incubated for 4-5 hours at 4°C with agitation. Charcoal is precipitated at 10800xg for 30 minutes at 4°C for two times as previously made. At the end, in the biological safety cabinet, the supernatant is vacuum filtered through a 0.45 uM sterile filter unit (Corning, polysytrene, cellulose acetate membrane, low protein binding). Charcoal dextran treated FBS is aliquoted into 50 ml falcon tubes and stored at -20°C .

This protocol is prepared by M. Muyan.